



JAAS

**A Multi-Electrode Glow Discharge Ionization Source for  
Atomic and Molecular Mass Spectrometry**

Journal:	<i>Journal of Analytical Atomic Spectrometry</i>
Manuscript ID	JA-ART-04-2020-000142.R1
Article Type:	Paper
Date Submitted by the Author:	03-May-2020
Complete List of Authors:	Hoegg, Edward; Clemson University, Department of Chemistry Williams, Tyler; Clemson University, Department of Chemistry Bills, Jacob; Clemson University, Department of Chemistry, Biosystems Research Complex Marcus, R.; Clemson University, Chemistry Koppenaar, David; Pacific Northwest National Laboratory, David Koppenaar; David Koppenaar

SCHOLARONE™  
Manuscripts

## A Multi-Electrode Glow Discharge Ionization Source for Atomic and Molecular Mass Spectrometry

Edward D. Hoegg, Tyler J. Williams, Jacob R. Bills, R. Kenneth Marcus, David W. Koppenaal

A novel multi-electrode glow discharge provides increased sensitivity and analytical flexibility for *both* atomic and molecular MS determinations.



# A Multi-Electrode Glow Discharge Ionization Source for Atomic and Molecular Mass Spectrometry

Edward D. Hoegg<sup>1a</sup>, Tyler J. Williams<sup>2</sup>, Jacob R. Bills<sup>2</sup>, R. Kenneth Marcus<sup>2</sup>, David W. Koppenaal<sup>1b\*</sup>

<sup>1</sup>National Security Directorate<sup>a</sup>, and EMSL<sup>b</sup>, Pacific Northwest National Laboratory, Richland WA 99353, USA.

\*Email: [david.koppenaal@pnnl.gov](mailto:david.koppenaal@pnnl.gov) or [dwk673@me.com](mailto:dwk673@me.com)

<sup>2</sup>Department of Chemistry, Biosystems Research Complex, Clemson University, Clemson, SC 29634, USA.

## Abstract

A new, multi-electrode, liquid sampling glow discharge ionization source for mass spectrometry is described. This ion source consists of multiple (2-4) counter (anode) electrodes in comparison to prior single counterelectrode designs of this type. In the experiments presented here these ion sources have been interfaced with ThermoScientific Exactive Orbitrap instruments and Advion Expression Compact Mass Spectrometer instruments. Advantages and analytical performance improvements are described. These include ability to use higher plasma currents, resulting in a more robust and energetic plasma exhibiting higher sensitivity, lower spectral background, ppt detection limits, and 2-3x faster washout times. A low-cost, 3D printed version of a dual counter electrode design is also described. The ion source can further be utilized in either atomic (elemental/isotopic) or molecular (molecular ion, fragmentation) ionization modes.

## Introduction

This contribution is presented in honor of the retirement of our colleague, mentor, and friend, Professor Gary M. Hieftje of Indiana University. Professor Hieftje's contributions to analytical chemistry in general and atomic spectroscopy in particular are legion. He is responsible for many fundamental insights and advances in flame and plasma spectrochemistry and mass spectrometry. He has been particularly innovative in the development of new instrumentation tools, one of the most prominent and effective ways to accelerate scientific knowledge and contributions. It is in this spirit that we describe this new, multi-electrode glow discharge ionization source for applications in both atomic and molecular mass spectrometry. We can think of no better way to honor

1  
2 Professor Hieftje than to promote and continue the development of new tools for  
3 extraordinary science.  
4

5 Elemental mass spectrometry (MS) has enjoyed continuous (albeit gradual)  
6 development of new ion sources over the century or so of its common use. From  
7 electron impact (EI) sources in the earliest days (pre-1950's), to arc and spark  
8 discharges (1950-1980's), and then to modern plasma ion sources (1980's-present),  
9 new ion source development has been critically important. Among these developments  
10 the use of the inductively coupled plasma (ICP) as an ionization source stands tall, as  
11 ICP-MS has dominated the field since the mid-1980's. Its principal advantages of high  
12 and uniform ionization yields enable the ultimate in sensitivity across the periodic table,  
13 and have driven elemental MS to new heights of use and application.  
14  
15  
16  
17  
18  
19  
20

21 Parallel ion source developments in the organic MS field have also occurred. The  
22 predominant ion sources developed include the EI source, electrospray ionization (ESI),  
23 and matrix-assisted laser desorption ionization (MALDI). Interestingly, the development  
24 of MS ion sources has proceeded along separate, broad organic/inorganic application  
25 pathways, with few (if any) common-use ion sources for both organic and  
26 inorganic/elemental MS use.  
27  
28  
29  
30

31 Along these lines, a new ion source capable of both organic and elemental  
32 ionization and analysis has been investigated by our research groups (Marcus/Clemson  
33 and Koppenaal/PNNL) over the last 9 years. This source, referred to as the liquid-  
34 sampling - atmospheric pressure glow discharge (LS-APGD) ion source, is a low-power  
35 (<50 W) microplasma (approximate size 1 mm<sup>3</sup>), that operates in the abnormal glow  
36 discharge regime and is capable of ionizing both molecular and elemental constituents  
37 under different operating conditions. First demonstrated as an elemental ion source in  
38 2011, this source was adapted from prior use as an optical emission (photon) source for  
39 elemental analysis (see a recent review for its history as both an optical emission  
40 source and a mass spectrometry ion source<sup>1</sup>). The first generation 'breadboard' LS-  
41 APGD ion source exhibited detection limits in the low ppb range and additionally  
42 provided isotope ratio measurement precision of better than 0.1% RSD.<sup>2-5</sup> A subsequent  
43 2<sup>nd</sup> generation 'production prototype' version has also been described and has exhibited  
44 even better analytical performance while providing users with an easily retrofittable ion  
45 source chamber that can interchange with many Orbitrap and other types of mass  
46 spectrometers.<sup>6</sup> Ionization in either soft (molecular, fragmentation spectra) or hard  
47  
48  
49  
50  
51  
52  
53  
54  
55  
56  
57  
58  
59  
60

(elemental, isotopic) modes, termed a combined atomic and molecular (CAM) ionization source, have been demonstrated. This aspect has in fact been used to demonstrate atomic mass resolution ( $R$ ) of over 1 M in a recent report.<sup>8</sup>

The early LS-APGD versions described above used a very simple single cathode/single anode electrode arrangement. This publication describes a novel variation of this design in which multiple (2,3, and 4) anode (counter) electrodes work in concert with a common liquid-carrying cathode electrode. We refer to this design as a multi-electrode LS-APGD, a 3<sup>rd</sup>-generation of the LS-APGD type. The rationale for adding additional electrodes was prompted by our experiences with increasing plasma power with higher operating currents using a single electrode (i.e., above 30-50 mA), in order to further increase sensitivity and analytical performance. At these higher current levels, the anode (counter electrode) tended to overheat and deform, leading to erratic plasma stability, operation, and even extinguishing of the plasma.<sup>1</sup> Additional counter electrodes allow for distribution of (higher) current among 2, 3, and 4 electrodes. Additional benefits include formation of a larger, more robust and powerful plasma that is capable of higher ionization efficiency and better sensitivity, as well as alleviating plasma positioning and alignment issues. In addition, engagement of multiple electrodes provides a novel level of plasma tunability for the ionization/fragmentation of polyatomic or molecular species/analytes. Development, construction, and improved performance attributes of this design are presented herein.

## **Experimental**

### *Source Design & Construction*

The original single-electrode LS-APGD MS ion source has been described in previous works.<sup>1-5</sup> The LS-APGD source operates by applying a potential between a nickel or stainless-steel counter (anode) counter-electrode (MDC Vacuum Products, LLC; Hayward, CA) and a grounded solution-carrying (cathode) electrode. A new design for the LS-APGD ion source has been developed that is more durable, robust, user friendly, and reliable. The electrodes have been integrated into a single piece/cartridge of aluminum, of a size slightly larger than a credit card (actual dimensions 10L x 8.4W x 0.75H cm), see Figure 1a. The solution is delivered to the plasma using a concentric capillary system in which the outer capillary (1 mm i.d., 6.35 mm o.d.) delivers a cooling

1  
2 He sheath gas, and an inner capillary (250  $\mu\text{m}$  i.d., 360  $\mu\text{m}$  o.d., Molex; Lisle, IL)  
3  
4 delivers solution to the plasma. The solution flow rate is controlled via a syringe pump  
5  
6 (Chemyx OEM 30020; Stafford, TX) and the gas flow is set via a mass flow controller  
7  
8 (Alicat BC-C1000-He-232-NPT). Both the counter electrodes and solution/gas flow  
9  
10 capillary/electrode are mounted in the card-sized aluminum block, which can be  
11  
12 conveniently and firmly mounted, manipulated, and aligned using a complementary  
13  
14 aluminum bracket with adjustment mechanisms. The plasma is ignited using a unique  
15  
16 auto ignition system (patent pending) that imposes a temporary, controlled high voltage  
17  
18 pulse sequence on the counter electrodes, resulting in instantaneous electron emission  
19  
20 and plasma formation. The plasma voltage is automatically reduced to a lower  
21  
22 operational voltage once the plasma is ignited and the preselected current established.  
23  
24 The plasma current is controlled using an Ultravolt high voltage power supply (1C24-  
25  
26 P60-I5, Ronkonkoma, NY). All controllers for plasma operation are housed in a  
27  
28 control/utility box designed and assembled by GAA Custom Electronics (Benton City,  
29  
30 WA). The unit consists of a 10 x 5 x 9" polycarbonate shell (Metcase; Bridgeville, PA),  
31  
32 and is controlled using a Raspberry Pi 3 – Model B (New York, NY) system with a 7"  
33  
34 diagonal resistive touchscreen display.

35  
36 Additional source designs employing multiple counter electrodes can be seen in  
37  
38 Figs 1b and 1c. We refer to these designs as dual-, tri-, or quad-electrode systems  
39  
40 based on the *number of counter electrodes* in the system (a common solution electrode  
41  
42 is employed in each case also). The dual-electrode design depicted in Fig 1b uses the  
43  
44 same components as the traditional single electrode design, albeit with the addition of a  
45  
46 second counter electrode with its own voltage source, with the solution electrode  
47  
48 operating at the common, ground. The counter electrodes in this configuration are co-  
49  
50 linear and placed perpendicular and equidistant to the solution electrode. The dual-  
51  
52 electrode design is conveniently amenable to the same aluminum card-based design  
53  
54 described above. The tri- and quad-electrode designs shown in Figure 1c also utilize the  
55  
56 same components as the other operating modes, but in this case are integrated into a  
57  
58 cross-based aluminum bracket mount design. This design adds the addition of either  
59  
60 one or two additional counter electrodes to the dual-electrode mode for a total of three  
or four counter electrodes. Voltages for all counter electrodes are supplied by separate,  
independent, current-controlled voltage supplies (ie the exact same current flows to each

1  
2 of the counter electrodes). Three of the power supplies used here were the Ultravolt  
3 model described earlier, while the fourth was a Glassman Model EH (High Bridge, NJ);  
4 a fourth Ultravolt supply was unavailable for these experiments and this was only  
5 reason for using the Glassman supply . Typical currents of between 25-50 mA are set  
6 and controlled for each counter electrode; this ensures a stable, centered plasma within  
7 the electrode axes region. In this way, additional electrodes provide greater current  
8 density in the plasma glow as well as added heating to affect the vaporization of the  
9 analyte-carrying electrolyte solution. There is no wandering or jumping of the plasma  
10 from one electrode to the other due to the controlled currents; the voltage changes  
11 observed are also insignificant. The system is switched between dual, tri, and quad  
12 electrode modes by simply turning one or more of the power supplies on/off. Future  
13 power supply designs, under design/development, will utilize a single integrated power  
14 supply capable of automated, multiplexed, and independent voltage channel operation,  
15 thus enabling use of a single as opposed to multiple separate supplies.  
16  
17  
18  
19  
20  
21  
22  
23  
24  
25

26  
27 In addition to the aluminum holder employed at PNNL, a 3D-printed LS-APGD  
28 was designed and fabricated at Clemson University out of polylactic acid filament on a  
29 Dremel 3D45 printer. The 3D printed model was outfitted with two MHV connectors,  
30 PEEK fittings for liquid lines, and stainless-steel fittings for gas lines. The electrodes  
31 were connected to the ground and “hot” portions of the MHV connector via internal  
32 connections. This design was engineered to be a replacement for the ESI source on an  
33 Advion (Ithaca, NY) Expression<sup>L</sup> Compact Mass Spectrometer (CMS). A diagram and  
34 photo of the 3D printed ion source is provided in Electronic Supplementary Information  
35 Figure 1 (ESI Fig. 1).  
36  
37  
38  
39  
40  
41  
42

### 43 *Mass Spectrometer Systems*

44

45 Experiments were carried out using three different mass spectrometer platforms.  
46 Proof of concept and initial feasibility studies for the operation of the LS-APGD with  
47 multiple electrodes was completed using a ThermoScientific (San Jose, CA) Exactive  
48 mass spectrometer at the Environmental Molecular Sciences Laboratory (EMSL) user  
49 facility at PNNL. The majority of the work comparing the single electrode and dual-  
50 electrode source designs was completed at Clemson University using a  
51  
52  
53  
54  
55  
56  
57  
58  
59  
60

1  
2 ThermoScientific Q Exactive Focus mass spectrometer and an Advion (Ithaca NY, USA)  
3 Expression<sup>L</sup> Compact Mass Spectrometer (CMS).  
4

5  
6 Interfacing with both Exactive MS platforms has been described previously and  
7 was completed by simply removing the commercial ESI source and attaching the  
8 plasma source, for which several mounting designs have been implemented and  
9 described previously.<sup>3-6</sup> In all system configurations, the solution electrode was mounted  
10 in-line with the sampling orifice with the counter electrodes mounted collinearly with  
11 each other, but perpendicular to the solution flow axis. Based on a brief optimization  
12 experiment, there was no modification, including changes to ion optic potentials or  
13 capillary temperatures, made to either Exactive platform. The instruments were  
14 operated in positive ion mode and, as in previous experiments, collision induced  
15 dissociation was used in order to limit any interfering molecular species. For these  
16 experiments, an in-source collision induced dissociation (CID) of 75 eV and a higher  
17 energy collision induced dissociation cell (HCD) voltage of 100 eV were used. In  
18 experiments conducted at Clemson University using the Q Exactive Focus, the  
19 quadrupole filter, located prior to the instrument's C-trap, was set to pass only ions of  
20 analytical interest into the C-trap (the C-trap serves to collect and compress the ion  
21 packet prior to injection into the Orbitrap mass analyzer).  
22  
23  
24  
25  
26  
27  
28  
29  
30  
31  
32  
33

34 The experiments completed with the Advion Expression<sup>TM</sup> Compact Mass  
35 Spectrometer (CMS) required little modification to the instrument and has been  
36 described in detail recently. Either single<sup>7</sup> or dual LS-APGD source designs were  
37 mounted inside the Advion source block for direct coupling to the instrument by simply  
38 removing the standard ESI source. Different from other instrument couplings, the LS-  
39 APGD is held at a 25° angle from the entrance into the mass spectrometer to mimic the  
40 angle of the instruments ESI source. Full scan data was acquired using a scan rate of  
41 500 ms across a mass range of 10-250 m/z and data collected using selected ion  
42 monitoring (SIM) used a mass window of 0.3 Da and a dwell time of 50 ms.  
43  
44  
45  
46  
47  
48  
49

### 50 *Test Samples & Standards*

51

52  
53 Experiments at PNNL were carried out using four test solutions. The first was a  
54 multi-element test solution containing Rb, Ag, Ba, Tl and U at a concentration of 500 ng  
55 mL<sup>-1</sup> each. Calibration solutions were made up of 1 ng mL<sup>-1</sup> - 10,000 ng mL<sup>-1</sup> containing  
56  
57  
58  
59  
60

1  
2 Cu, Cs, and Pb. In order to test the ability to make high precision isotope ratio  
3 measurements a 500 ng mL<sup>-1</sup> U solution of natural isotopic abundance was prepared.  
4 Finally, a multi-element solution containing Cu, Rb, Ag, Cs, Ba, Pb, Tl, and U was  
5 prepared at a concentration of 500 ng mL<sup>-1</sup> each. Evaluation of the dual-electrode  
6 design on the CMS utilized two multi element solutions, one containing Rb, Cs, and Tl,  
7 and the other containing Ca, Mg, Cu, K, Na, Pb, Zn, Fe, and Cd. Calibration solutions  
8 for the first solution ranged from 50 ng mL<sup>-1</sup> to 10,000 ng mL<sup>-1</sup> of each element, and for  
9 the second solution ranged from 500 pg mL<sup>-1</sup> to 1000 ng mL<sup>-1</sup> of each element.  
10  
11  
12  
13  
14  
15

16  
17 Organic samples were prepared in a 70:30 MeOH:H<sub>2</sub>O mixture. The solvent  
18 mixture was prepared using methanol (HPLC grade, EMD Millipore, Billerica MA) and  
19 18.2 MΩ cm<sup>-1</sup> deionized water from an Elga PURELAB flex water purification system  
20 (Veolia Water Technologies, High Wycombe, England). Caffeine was obtained from  
21 Aldrich chemical company (St. Louis, MO) and triethyl phosphate was obtained from  
22 Alfa Aesar (Ward Hill, MA). Both were dissolved in the 70:30 MeOH:H<sub>2</sub>O mixture at a  
23 concentration of 1 μg mL<sup>-1</sup>. The samples were introduced into the ionization source  
24 using the MeOH:H<sub>2</sub>O mixture as the mobile phase and introducing the sample in discrete  
25 20 μL injections.  
26  
27  
28  
29  
30  
31

## 32 **Results and Discussion**

33  
34 To compare the single and dual electrode designs, preliminary experiments were  
35 completed at both PNNL (ThermoScientific Exactive) and Clemson (ThermoScientific Q-  
36 Exactive). The first experiments looked at the current-voltage (i-V) relationships of the  
37 two designs and the second examined ion intensity/signal comparisons.  
38  
39  
40  
41

### 42 *Plasma Operation and Operating Regimes*

43  
44  
45 Glow discharges, such as the LS-APGD, are defined by the i-V relationships for a  
46 given plasma size, across their operating regimes. Given the changes made in these  
47 designs, confidence was needed that operation in a glow discharge regime was  
48 maintained. Accordingly, i-V plots were generated (Fig. 2) where the discharge  
49 maintenance voltage is plotted for the current imposed on each electrode; whether  
50 single or double. The results of the current voltage plot generated by the single  
51 electrode design show a very slightly positive slope which corresponds with the  
52 abnormal glow discharge regime, consistent with previous studies<sup>1</sup>. The low extent of a  
53  
54  
55  
56  
57  
58  
59  
60

1  
2 positive slope is attributed to an increase in the plasma volume as the current  
3  
4 increases. Previous studies used a glass sleeve to limit the contact area that the plasma  
5  
6 had with the counter electrode, this glass sleeve has been removed in recent designs to  
7  
8 limit carryover and simplify operation, however, without the glass sleeve, the plasma  
9  
10 grows in size as the current is increased. With the dual-electrode design, there is an  
11  
12 initial slight increase in the total voltage (the sum of the two individual supplies) as the  
13  
14 current is increased, but at the highest current, beyond which a slight drop is seen. Here  
15  
16 again, the plasma is getting visibly larger when dual counter electrodes are operated at  
17  
18 higher currents. Somewhat surprising in this data is the fact that there appears to be no  
19  
20 sort of cooperative effects in the case of the dual-electrode system. It had been  
21  
22 expected that there might be a lessening of the total required voltage, with the increase  
23  
24 seen being reflective of the slightly larger interelectrode spacing. The drop in potential at  
25  
26 the 50 mA (each) current may be some indication of cooperativity, but beyond this point  
27  
28 the system suffers from electrode overheating. The general trends suggest that  
29  
30 *electrically* two different plasmas are operating with a common cathode (an interesting  
31  
32 observation that might be used to advantage but requires further investigation). As will  
33  
34 be seen in the subsequent mass spectrometric responses, the net effects are indeed a  
35  
36 reflection of greater amounts ( $\geq 2X$ ) of overall power in the plasma. Future experiments  
37  
38 that might possibly restrain the plasma size are necessary to obtain a truly valid  
39  
40 comparison. However, the initial voltage ramp results indicate that the dual electrode  
41  
42 plasma is likely operating in a similar glow discharge regime as the single.

### 43 *Analyte ion and background improvements*

44  
45 The single counter electrode source geometry has been used as an ionization  
46  
47 source for mass spectrometry since 2011,<sup>2</sup> when it was first interfaced with a  
48  
49 ThermoScientific Exactive MS. It was reasoned that a larger and more powerful plasma  
50  
51 would provide an improvement in ion production, sensitivity, and other analytical figures  
52  
53 of merit, and that a simple way to obtain such an improvement would be the addition of  
54  
55 plasma current via additional electrodes. Previous attempts at providing more current  
56  
57 with a single electrode showed inconsistent and sporadic results owing to electrode  
58  
59 heating, deformation, and even destruction<sup>1</sup>. Using separate electrodes carrying  
60  
61 additional current resolves the overheating issues, effectively spreading the current. It  
62  
63 additionally provides for a larger and more robust plasma, likely alleviating sensitivity to

1  
2 positioning and alignment. Comparison of improvements with a dual electrode system  
3 was completed using a multi-element solution containing 500 ng mL<sup>-1</sup> each of Rb, Ag,  
4 Ba, Tl and U. Spectra (presented as ESI Fig. 2a-d) show signal intensity improvements  
5 (up to 150X) with the dual electrode system in comparison to the single electrode  
6 system, depending on element. When a wide digitization range is used, Rb is the  
7 dominant ion in the spectra and an approximate increase of 6x is observed comparing  
8 the two designs. When Rb is removed from the Orbitrap acquisition using a narrower  
9 digitization window, Fig 2c and d, a 17X improvement in sensitivity is observed for Ag,  
10 and an improvement of over 175X is observed for Ba in comparison to the single  
11 electrode system. Similar improvements in response are seen for Tl and UO<sub>2</sub>. The  
12 differences in the level of enhancement reflect their improved efficiencies between the  
13 two operation modes. This improved efficiency is also observed in the ion collection  
14 time of the orbitrap. During the experiments the maximum injection time (collection time)  
15 was set to 100 msec. When the single electrode design was used, the injection time  
16 was 100 msec. When the dual electrode was employed not only was the signal intensity  
17 improved, but the injection time was only 64 msec for an average of 10 scans signifying  
18 an increase in the number of ions being generated, ie a higher ionization efficiency.  
19  
20  
21  
22  
23  
24  
25  
26  
27  
28  
29  
30

31  
32 An additional advantage with the dual electrode system is observed in  
33 background intensities. Significantly fewer molecular background/concomitant ions are  
34 observed in the dual electrode system. This advantage can manifest itself in better  
35 detection limits and improved sensitivity and precision. The reduction in the number of  
36 background molecular ions is likely caused by the higher power and temperatures which  
37 leads to greater fragmentation and destruction of concomitant molecular species.  
38 Previous studies using the single electrode LS-APGD showed that these background  
39 ions are typically solvent-related clusters, taking the general form of (H<sub>2</sub>O)<sub>n</sub>H<sup>+</sup>, or  
40 perhaps hydrated metal ion forms of these solvent clusters.<sup>2</sup>  
41  
42  
43  
44  
45  
46  
47

48 A similar set of experiments was run at Clemson University using the Advion  
49 Expression<sup>l</sup> Compact Mass Spectrometer (CMS). This instrument is a small, lower-  
50 overhead quadrupole MS for laboratory or field-portable applications. A multi-element  
51 solution containing Rb, Cs, and Tl at a concentration of 10 µg mL<sup>-1</sup> each was used to  
52 again examine analyte species and background characteristics of the ion source with  
53 this MS system. The first experiment considered the ability of the dual-electrode  
54  
55  
56  
57  
58  
59  
60

1  
2 configuration to reduce the number of molecular background ions, as would be most  
3 beneficial on the quadrupole analyzer instrument. As seen in Fig. 3, when the spectrum  
4 generated using the single electrode operating at 30 mA is overlaid with the spectrum  
5 generated using the dual-electrode of 30 mA each, there is a significant increase in  
6 response, as well as a significant decrease in the number and intensity of background  
7 ions when using the dual-electrode design. In this case, each of the metals shows an  
8 ~4x improvement, while discrete solvent-related background peaks drop in intensity to  
9 even greater extents. For example, the ratio of the  $^{133}\text{Cs}$  to an adjacent background ion  
10 at  $m/z = 135$  Da (equivalent to a species of the form  $(\text{H}_2\text{O})_4\text{NO}_3\text{H}^+$ ), increases from 18  
11 to 262.  
12  
13  
14  
15  
16  
17  
18  
19

20 A new, interesting observation was made during the CMS experiments regarding  
21 washout times. This is the time it takes for the signal to return to baseline after (or  
22 between) analyte injections. Washout times were significantly reduced for the dual-  
23 electrode system compared to the single electrode system. Figures 4a and 4b show the  
24 signal transients of a 20  $\mu\text{L}$  injection of 10  $\mu\text{g mL}^{-1}$  Rb sample for the two powering  
25 modes. In principle, the injection peak should be ~40 s wide, though longitudinal  
26 diffusion broadening would add somewhat to that. Both transients do indeed reflect the  
27 expected general shape. Closer inspection of the trailing edges of the transient reveals  
28 that the single electrode does not reach the pre-injection level until approximately 190 s  
29 after the initial injection pulse, while the complete washout time for the dual-electrode  
30 case is ~90 s. It is hypothesized that the increased energy, plasma temperature, and  
31 the operating distance between the microplasma and the sampling orifice decreases  
32 analyte deposition there, associated memory effects, and resulting background levels.  
33 With the single-electrode system, the plasma is operated at a distance of about 1 mm  
34 from the MS orifice while for the dual-electrode design it can be operated farther away  
35 (up to ~40 mm) from the orifice with better sensitivity. This again indicates an analytical  
36 advantage for the dual- or other multi-electrode systems.  
37  
38  
39  
40  
41  
42  
43  
44  
45  
46  
47  
48  
49

### 50 *Limits of Detection*

51  
52 The differences in detection limits between the single- and dual-electrode  
53 configurations were quantified using a ThermoScientific Q Exactive Focus, located at  
54 Clemson University, and were measured using a multi-element solution containing, Cu,  
55  
56  
57  
58  
59  
60

1  
2 Cs, and Pb. Solutions were diluted to generate response curves that cover a 5 orders-  
3 of-magnitude concentration range. While the solution contained multiple elements each  
4 one was observed individually by using the quadrupole mass filter to select analyte ion  
5 mass ranges passed into the C-trap/Orbitrap. Additionally, a narrow  
6 acquisition/digitization range was used to further select said ions. While Cs is  
7 monoisotopic, for Cu and Pb, where multiple isotopes are present and thus  
8 simultaneously measured by the Orbitrap, only  $^{65}\text{Cu}$  and  $^{204}\text{Pb}$  were plotted. The  
9 response curves for each element/isotope are plotted in ESI Figs. 3a-c, where each  
10 data point represents 3 injections of 100  $\mu\text{L}$  each. For most cases the error bars are  
11 smaller than the data point itself. In these experiments, the single electrode and each  
12 electrode of the dual-electrode designs were operated at 30 mA.

13  
14 A natural question arises as to whether there is a difference between running two  
15 counter electrodes at 30 mA each or running a single counter electrode at 60 mA (total  
16 of 60 mA powering the plasma in both cases). Experiments were accordingly also run to  
17 address this question and for comparison to the other analytical modes (see again ESI  
18 Figs. 3a-c). In the case of Cu and Pb, there is an order of magnitude improvement for  
19 both the raw responses and limits of detection when comparing the dual 30 mA  
20 electrode results to the 30mA single electrode. The dual 30 mA dual electrode system  
21 also outperforms the 60 mA single electrode system, although the 60 mA single  
22 electrode system offers improved performance over the 30 mA single electrode system.  
23 When analyzing Cs, using the single electrode system at both 30 mA and 60 mA, the  
24 response curves become non-linear at the high concentration range ( $>1,000 \text{ ng mL}^{-1}$ ).  
25 This was not seen for either Cu or Pb even when the most abundant isotope was  
26 plotted instead. This response was not seen when using the dual-electrode for any of  
27 the samples tested, which suggests that ionization limits may be reached for the easily-  
28 ionized Cs at high solution concentrations with the single-electrode design. This, along  
29 with the signal response improvement when using the dual-electrode system, suggests  
30 that the ionization efficacy of the dual-electrode system is greater than that of the single  
31 electrode system.

32  
33 Based on these response curves, limit of detection (LOD) values were calculated  
34 for each element and microplasma powering condition, Table 1. LOD figures were  
35 calculated using the equation

$$LOD = \frac{3\sigma}{m}$$

where  $\sigma$  is the standard deviation of the lowest concentration value,  $m$  is the slope of the line, and a multiplier of  $k=3$  is used, representing a 99% confidence interval. In the case of Cs the LOD is at the 2 ppt level, with both Cu and Pb having values that extend >3X lower when using the dual-electrode design. When the absolute-mass detection limit is calculated for each of these elements, the quantity ranges from tens to hundreds of femtograms, an impressive performance considering the low (100  $\mu$ L sample volumes used).

Sensitivity and LOD experiments were again run using both the 30 mA single electrode and the dual 30 mA electrode systems on the CMS quadrupole instrument. The data was taken using triplicate injections, 20  $\mu$ L each, of the multi-element solution, diluted to cover 4+ orders of magnitude, 500  $\text{pg mL}^{-1}$  to 1000  $\text{ng mL}^{-1}$ . The CMS system was operated in selected ion monitoring (SIM) mode with a mass range centered on the most abundant isotope of each element with a mass range of 0.3 Da and a dwell time of 50 ms. Table 2 compares the results from this study and shows nearly universal improvement in the calculated LODs when using the dual-electrode system, with only Ca curiously breaking the trend. In this instance, and also the case for Na and K, the presence of molecular isobars is the likely limiting feature. That said, a significant decrease in the number of background ions when using the dual-electrode system compared to the single-electrode system was again observed in these experiments. While the CMS system is clearly less sensitive than the Orbitrap MS system, the results are still impressive for this low cost and small footprint system.

### *Isotope Ratio Measurement Precision*

One of the more interesting applications of the LS-APGD has been as a new ionization source for measuring isotope ratios when coupled with orbitrap mass spectrometers. Our work,<sup>3-5</sup> as well as that of Eiler and colleagues (low mass stable isotope and oxyanion isotope ratio work),<sup>11-14</sup> indicate that excellent analytical ratio precision can be achieved with Orbitrap MS systems, contrary to conventional wisdom. Although our research is relatively recent, it has already met or exceeded traditional elemental mass spectrometer performance when measuring U or other isotope ratios.<sup>3-5</sup>

1  
2 By harnessing the resolving power of orbitrap instruments, it is also possible to measure  
3 isotope ratios of samples, even those that typically suffer from interelement isobaric  
4 interferences. In order to show that there is no degradation of performance when  
5 performing high precision isotope ratio measurements using the dual-electrode ion  
6 source, a test solution containing CRM-129a ( $^{235}\text{U}/^{238}\text{U} = 0.0072614$ ) was analyzed  
7 (Table 3). When these results are compared to measurements taken using the single  
8 electrode, the measurement precision remains excellent, with no statistical difference  
9 observed. There is however a slight improvement in the accuracy with the dual-  
10 electrode system. This is most likely due to the reduction of background ions that lead  
11 to the noise levels (even though the noise level is lowered by software treatment in the  
12 Exactive MS system, see earlier work by our group<sup>3-6</sup>). Note that these values are not  
13 corrected for mass bias, which is typical with many other MS systems. When compared  
14 to the International Target Values (ITV) for Measurement Uncertainties in Safeguarding  
15 Nuclear Materials,<sup>15</sup> the uncertainty measured here falls below the acceptable random  
16 uncertainty component of the ITV, as had previous single-electrode efforts.<sup>16-17</sup>

### 27 *Molecular Species Analysis*

28  
29  
30  
31 While the LS-APGD was originally implemented as an atomic ion source, it has  
32 been shown as a viable ion source for molecular analysis as well. This is accomplished  
33 by simply changing the sample preparation to use an organic solvent, such as a  
34 MeOH:H<sub>2</sub>O solution, which effectively “cools down” the plasma which yields molecular  
35 mass spectra with a high degree of information about the compound. Previous studies  
36 have shown that the discharge current, and resulting number of available electrons  
37 generated, corresponds with the amount of fragmentation with high currents yielding  
38 more fragmentation.<sup>3,10</sup> By doubling the power density of the plasma, the resulting  
39 electron density will be higher suggesting a greater degree of ionization/fragmentation.  
40 The concept of using single and dual electrode operation to affect predominately  
41 chemical ionization (CI) versus electron ionization (EI) spectral features is illustrated in  
42 Figs. 5a and b. In this case, the common organic mass spectrometry standard, caffeine  
43 and triethyl phosphate (a chemical warfare simulant), are used as demonstrations,  
44 respectively. These samples were run as discrete 20  $\mu\text{L}$  injections on the Advion CMS  
45 using the 3D-printed LS-APGD ion source. As can be seen, the mass spectra obtained  
46 using the single electrodes are very much akin to chemical ionization sources, where  
47  
48  
49  
50  
51  
52  
53  
54  
55  
56  
57  
58  
59  
60

1  
2 proton donation yields large amounts of the  $(M+H)^+$  pseudo-molecular ion, where the  
3 dual electrode results in a larger degree of fragmentation for both compounds. Similar to  
4 the atomic analysis presented above, the number of solvent-related background ions is  
5 also reduced when using the dual electrode source. Further investigation is required to  
6 deduce and optimize the exact ionization mechanisms and resulting fragmentation  
7 pathways. However, an advantage of the multi-electrode LS-APGD system is that one  
8 could rapidly pulse (ms) the second counter electrode to produce alternating CI/EI  
9 spectra on time scales of relevance for liquid chromatography elution peaks. In this way,  
10 a single quadrupole analyzer could affect many of the desired functions of triple-  
11 quadrupole instruments.

### 12 *Tri- and Quad-Electrode Systems*

13  
14 In an effort to further improve the LS-APGD performance, experiments focused  
15 on increasing the number of counter electrodes were conducted at PNNL. A multi-  
16 element solution containing  $500 \text{ ng mL}^{-1}$  of Cu, Rb, Ag, Cs, Ba, Pb, and U was analyzed  
17 using a dual-electrode, tri-electrode, and quad-electrode LS-APGD configuration, as  
18 described in the Experimental Section and Fig. 1c above. Results are shown in Figs.  
19 6a-c, where an approximate order of magnitude increase for Rb, Ag, and Cs ion  
20 intensities is observed as each additional plasma counter electrode is engaged. The  
21 previous studies comparing the single and dual electrodes observed a decrease in the  
22 recorded ion injection times on the Orbitrap in the latter case, owing to higher ion  
23 currents. In the studies that compared the dual, tri, and quad electrode designs, a  
24 decrease was only observed when using the quad electrode, a 77 msec average  
25 injection time for 10 scans. For the dual and tri electrode systems the injection time was  
26 recorded to be 100 msec, the maximum allowable injection time for these experiments.  
27 Additionally while there was improvement between the dual, tri, and quad electrode  
28 systems, the sensitivity of the dual electrode system is a factor of 10 less in these  
29 experiments than those presented above, reflecting some variance between  
30 experiments. Given the increase in sensitivity, and the normal voltage observed on each  
31 of the power supplies during the experiments it is not like that the problem is with the ion  
32 source but rather with the interface or the MS itself. In fact in later servicing of the  
33 instrument it was observed that the ion source inlet had significant soot built up on the  
34 ion optics reducing the ion transmission efficiency. This suggests that an even greater

1  
2 improvement may be realized in future experiments. At the same time, while perhaps  
3 not of an issue with the outstanding mass resolving power of the Orbitrap, the spectral  
4 background species become effectively non-existent.  
5  
6

7  
8 The physical characteristics of the multi-electrode plasma of course change  
9 significantly. The size and shape of the plasma increases with addition of  
10 counterelectrodes, to the point with the quad-electrode system that the plasma adopts a  
11 tail flame of sorts with an appearance akin to a mini-ICP (see photograph, Fig. 7). In this  
12 case the primary plasma is a coalesced, 4x cylindrical-to-spherical/toroidal, shape of  
13 nominal 3 x 3 mm cross-sectional size (not including tail flame). This quad electrode  
14 configuration has the benefit of being used as a single-, dual-, tri-, or quad electrode  
15 system according to sensitivity or other analytical needs. This configuration allows  
16 active, or “hot”, selection of the single/dual/tri/quad modes (i.e., the plasma can be  
17 increased or decreased in power by simply powering or de-powering each electrode  
18 sequentially). This feature may have future advantage for selective ionization of certain  
19 elements, use or avoidance of interferent ions, or use in a combined atomic or  
20 molecular analysis mode, results of which will be reported in a subsequent work. It is  
21 also presumed that designs using additional multi-electrodes might result in even better  
22 performance.  
23  
24  
25  
26  
27  
28  
29  
30  
31  
32  
33

## 34 **Conclusion**

35  
36 A new multi-electrode LS-APGD ion source has been demonstrated to show  
37 significant analytical advantages for both elemental and molecular mass spectrometry.  
38 In the atomic mode, increased analyte ion yields (approximately an order of magnitude  
39 improvement for each counter electrode added) and lower detection limits are achieved.  
40 In addition, spectral background contributions and analyte washout (memory) times are  
41 reduced. These improvements are due to higher plasma powers (and likely  
42 temperatures) being achieved with the multi-electrode design. In the molecular mode,  
43 using multiple electrodes also shows higher degrees of ionization and fragmentation,  
44 indicating that this source can be capable of both soft and hard ionization modes. A key  
45 development in the course of this work is the ability to assemble LS-APGD sources of  
46 various geometries using straight forward 3D printing techniques. At this point,  
47 materials costs for the source bodies, exclusive of commercial high voltage  
48  
49  
50  
51  
52  
53  
54  
55  
56  
57  
58  
59  
60

1  
2 feedthroughs and the like, are less than \$10 per device. Future work will seek to  
3 demonstrate the efficacy of this ion source for specific applications, and there are many  
4 fundamental questions to be addressed in terms of the coupling of higher power  
5 densities into the microplasma. This work demonstrates a significant addition to the  
6 repertoire of available ion sources for mass spectrometry, and it is hoped that this  
7 development will spur adoption and additional investigations and applications by new  
8 research groups and instrument manufacturers. A US patent covering portions of this  
9 work is pending.  
10  
11  
12  
13  
14  
15  
16  
17  
18

## 19 Acknowledgements

20  
21 This research was performed and supported by Pacific Northwest National  
22 Laboratory, a multi-program national laboratory operated by Battelle for the U.S.  
23 Department of Energy under Contract DE-AC05-76RL01830. The Exactive Plus MS  
24 experimental work was performed at the W. R. Wiley Environmental Molecular Science  
25 Laboratory (EMSL), a national scientific user facility sponsored by the U.S. Department  
26 of Energy's Office of Biological and Environmental Research (BER) program. PNNL  
27 support was in form of LDRD funding. The Clemson University portions of this effort were  
28 supported through a collaboration with Advion Inc.  
29  
30  
31  
32  
33  
34  
35  
36  
37  
38  
39  
40

## 41 References

- 42 1. R.K. Marcus, B.T. Marnard, C.D. Quarles Jr., *J. Anal. At. Spectrom.*, 2017, **32**, 704-716.
- 43 2. R. K. Marcus, C. D. Quarles, C. J. Barinaga, A. J. Carado, D. W. Koppenaal, *Anal. Chem.*, 2011,  
44 **83**, 2425–2429
- 45 3. C.D. Quarles Jr., A.J. Carado, C.J. Barinaga, D.W. Koppenaal, R.K. Marcus, *Anal Bioanal Chem.*,  
46 2012, **402**, 261–268
- 47 4. E. D. Hoegg, C. J. Barinaga, G. J. Hager, G. L. Hart, D. W. Koppenaal, R. K. Marcus, *J. Am. Soc.*  
48 *Mass Spectrom.*, 2016, **27**, 1393-1403
- 49 5. E. D. Hoegg, C. J. Barinaga, G. J. Hager, G. L. Hart, D. W. Koppenaal, R. K. Marcus, *J. Anal. At.*  
50 *Spectrom.*, 2016, **31**, 2355-2362
- 51 6. E.D. Hoegg, S. Godin, J. Szpunar, R. Lobinski, D.W. Koppenaal, R. K. Marcus, *J. Anal. At.*  
52 *Spectrom.*, 2019, **34**, 1387-1395.
- 53 7. T. J. Williams and R. K. Marcus, *J. Anal. At. Spectrom.*, 2020, submitted.
- 54 8. E. D. Hoegg, S. Godin, J. Szpunar, R. Lobinski, D. W. Koppenaal, R. K. Marcus, *J. Am. Soc.*  
55 *Mass Spectrom.*, 2019, **30**, 1163-1168.

- 1
  - 2
  - 3
  - 4
  - 5
  - 6
  - 7
  - 8
  - 9
  - 10
  - 11
  - 12
  - 13
  - 14
  - 15
  - 16
  - 17
  - 18
  - 19
  - 20
  - 21
  - 22
  - 23
  - 24
  - 25
  - 26
  - 27
  - 28
  - 29
  - 30
  - 31
  - 32
  - 33
  - 34
  - 35
  - 36
  - 37
  - 38
  - 39
  - 40
  - 41
  - 42
  - 43
  - 44
  - 45
  - 46
  - 47
  - 48
  - 49
  - 50
  - 51
  - 52
  - 53
  - 54
  - 55
  - 56
  - 57
  - 58
  - 59
  - 60
9. L.X. Zhang, R.K. Marcus, *J. Anal. At. Spectrom.* 2016, **31**, 145 – 151.
10. L. X. Zhang, B. T. Manard, B. A. Powell, R. K. Marcus, *Anal. Chem.*, 2015, **87**, 7218-7225.
11. C. Neubauer, M.J. Sweredoski, A. Moradian, D.K. Newman, R.J. Robins, J.M. Eiler, *Int. J. Mass Spectrom.* 2018, **434**, 276– 286.
12. C. Neubauer, A.L. Sessions, I.R. Booth, B.P. Bowen, S.H. Kopf, D.K. Newman, N.F. Dalleska, , J.M. Eiler, *Rapid Commun. Mass Spectrom.* 2018, **32**, 2129–2140.
13. J. Eiler, J. Cesar, L. Chimiak, B. Dallas, K. Grice, J. Griep- Raming, D. Juchelka, N. Kitchen, M. Lloyd, A. Makarov, et al. *Int. J. Mass Spectrom.* 2017, **422**, 126–142.
14. C Neubauer, A Cremiere, XT Wang, N Thiagarajan, AL Sessions, JF Adkins, NF Dalleska, AV Turchyn, JA Clegg, A Moradian, MJ Sweredoski, SD Garbis, JM Eiler, *Anal. Chem.*, <https://dx.doi.org/10.1021/acs.analchem.9b04486>
15. K. Zhao, M. Penkin, C. Norman, S. Balsley, K. Maryer, P. Peerani, C. Pietri, S. Tapodi, Y. Tsutaki, M. Boella, G. Renha and E. Huhn, International Target Values 2010 for Measurement Uncertainties in Safeguarding Nuclear Materials, 2010.
16. E.D. Hoegg, R.K. Marcus, D. W. Koppenaar, J. Irvahn, G. J. Hager and G. L. Hart, *Rapid Commun. in Mass Spectrom.*, 2017, **31**, 1534-1540
17. E. D. Hoegg, B. T. Manard, E. M. Wylie, K. J. Mathew, C. F. Ottenfeld and R. K. Marcus, *J. Am. Soc. Mass Spectrom.*, 2019, **30**, 278-288.

Table 1. Comparison of single vs dual electrode LS-APGD results. Single electrode held at either 30 mA or 60 mA; Dual electrodes held at 30 mA (each). 100 mL injections. Exactive Orbitrap MS system utilized.

Electrode Configuration	(Isotope)	(ng mL <sup>-1</sup> )	(pg)
<b>Dual Electrode (30 mA)</b>		<b>0.00068</b>	<b>0.07</b>
Single Electrode (60 mA)	<sup>65</sup> Cu	0.02249	2.25
Single Electrode (30 mA)		0.09864	9.86
<b>Dual Electrode (30 mA)</b>		<b>0.00217</b>	<b>0.22</b>
Single Electrode (60 mA)	<sup>133</sup> Cs	0.01062	1.06
Single Electrode (30 mA)		0.01443	1.44
<b>Dual Electrode (30 mA)</b>		<b>0.00068</b>	<b>0.07</b>
Single Electrode (60 mA)	<sup>204</sup> Pb	0.00563	0.56
Single Electrode (30 mA)		0.01180	1.18

Table 2. Comparison of single vs dual electrode LS-APGD LOD's. Single electrode held at 30 mA and dual electrodes held at 30 mA (each). 10 mL injection. Advion Expression<sup>TM</sup> CMS system utilized.

<b>Element</b>	<b>Single Electrode (ng mL<sup>-1</sup>)</b>	<b>Dual Electrode (ng mL<sup>-1</sup>)</b>	<b>Dual Electrode (ng)</b>
<b>Na</b>	<b>424</b>	<b>134</b>	<b>1</b>
<b>Mg</b>	<b>500</b>	<b>6</b>	<b>0.06</b>
<b>K</b>	<b>797</b>	<b>103</b>	<b>1</b>
<b>Ca</b>	<b>35</b>	<b>50</b>	<b>0.5</b>
<b>Fe</b>	<b>310</b>	<b>72</b>	<b>0.7</b>
<b>Cu</b>	<b>140</b>	<b>66</b>	<b>0.7</b>
<b>Zn</b>	<b>948</b>	<b>26</b>	<b>0.3</b>
<b>Rb</b>	<b>28</b>	<b>2</b>	<b>0.02</b>
<b>Cd</b>	<b>106</b>	<b>0.5</b>	<b>0.005</b>
<b>Cs</b>	<b>18</b>	<b>5</b>	<b>0.05</b>
<b>Tl</b>	<b>20</b>	<b>6</b>	<b>0.06</b>
<b>Pb</b>	<b>128</b>	<b>24</b>	<b>0.2</b>

Table 3. Comparison of  $^{235}\text{U}/^{238}\text{U}$  isotope ratio measurements using single vs dual electrode LS-APGD ion source with Exactive MS system.

	<b>Single Electrode</b>	<b>Dual Electrode</b>
<b>Average</b>	<b>0.006802</b>	<b>0.006855</b>
<b>Std Dev</b>	<b>5.2E-06</b>	<b>3.9E-06</b>
<b>%RSD</b>	<b>0.076</b>	<b>0.057</b>

## Figure Captions

Figure 1. a) New LS-APGD design showing electrodes along with electrical and solution connections integrated into a compact, solid aluminum card/cartridge. This card can be easily mounted, manipulated, and deconstructed/rebuilt. b) Dual-electrode design with two counter electrodes. c) Quad electrode design with up to 4 counter electrodes, using a cross-shaped variant of the card design.

Figure 2. Current-voltage plot for the new LS-APGD dual-electrode design compared to the traditional single electrode design, both affected on the aluminum card source assembly. Solvent = 2 % HNO<sub>3</sub>, solution flow rate 30 μL min<sup>-1</sup>, He sheath flow = 0.5 L min<sup>-1</sup>.

Figure 3. Comparison of single- vs dual-electrode signal response for elements Rb, Cs, and Tl, showing ~3-5x increased signal response for dual-electrode LS-APGD, using Advion Expression<sup>L</sup> CMS system.

Figure 4. Rb signal washout times for single (a) vs dual (b) electrode LS-APGD runs using Advion Expression<sup>L</sup> CMS system. Faster washout by ~3.5x is noted for the dual electrode source.

Figure 5. Molecular spectra for caffeine (a) and triethyl phosphate (b) acquired using single and dual electrode 3D printed LS-APGD ion source, Advion Expression<sup>L</sup> MS. Note higher fragmentation levels and decreased background with dual electrode ion source use.

Figure 6. Cu, Rb, Ag, Cs, Ba, Pb, and U intensity plots for dual (a), tri (b), and quad (c) electrode LS-APGD runs using Exactive Orbitrap MS system. An approximate 10x increase is observed with addition of each counter electrode.

Figure 7. Photograph of quad-electrode LS-APGD ion source, showing 4 counter electrodes in vertical axis, along with horizontal solution electrode and ion sampling capillary of PNNL/EMSL Exactive Orbitrap MS.

**Electronic Supplementary Information – Figure Captions**

Electronic Supplementary Information Figure 1. Photograph of 3D-printed LS-APGD dual-electrode ion source. This ion source was used in Advion Expression Compact MS experiments.

Electronic Supplementary Information Figure 2. Spectra of a multi-element solution containing 500 ng mL<sup>-1</sup> of Rb, Ag, Ba, Tl and U taken using the single and dual electrode designs on a Q Exactive Orbitrap mass spectrometer. A) Single electrode LS-APGD and a wide digitization range, B) dual electrode LS-APGD and a wide digitization range, C) Single electrode LS-APGD and a narrow digitization range, d) dual electrode LS-APGD and a narrow digitization range. Wide digitization range includes Rb ions, narrow range excludes Rb ions.

Electronic Supplementary Information Figure 3. Response curves generated using the single electrode design operated at 30 and 60 mA and the dual electrode design with each electrode operated at 30 mA. Three elements were analyzed, and the minor isotope was plotted; A) <sup>204</sup>Pb, B) <sup>65</sup>Cu, and C) Cs.

---

# Multi Electrode Paper, Koppenaal

## Figure Legends

1  
2  
3  
4  
5  
6  
7  
8  
9  
10  
Figure 1. a) New LS-APGD design showing electrodes along with electrical and solution connections integrated into a compact, solid aluminum card/cartridge. This card can be easily mounted, manipulated, and deconstructed/rebuilt. b) Dual-electrode design with two counter electrodes. c) Quad electrode design with up to 4 counter electrodes, using a cross-shaped variant of the card design.

11  
12  
13  
14  
15  
Figure 2. Current-voltage plot for the new LS-APGD dual-electrode design compared to the traditional single electrode design, both affected on the aluminum card source assembly. Solvent = 2 % HNO<sub>3</sub>, solution flow rate 30 mL min<sup>-1</sup>, He sheath flow = 0.5 L min<sup>-1</sup>.

16  
17  
18  
19  
Figure 3. Comparison of single- vs dual-electrode signal response for elements Rb, Cs, and Tl, showing ~3-5x increased signal response for dual-electrode LS-APGD, using Advion Expression CMS system.

20  
21  
22  
23  
Figure 4. Rb signal washout times for single (a) vs dual (b) electrode LS-APGD runs using Advion Expression CMS system. Faster washout by ~3.5x is noted for the dual electrode source.

24  
25  
26  
27  
28  
29  
Figure 5. Molecular spectra for caffeine (a) and triethyl phosphate (b) acquired using single and dual electrode 3D printed LS-APGD ion source, Advion Expression MS. Note higher fragmentation levels and decreased background with dual electrode ion source use.

30  
31  
32  
33  
Figure 6. Cu, Rb, Ag, Cs, Ba, Pb, and U intensity plots for dual (a), tri (b), and quad (c) electrode LS-APGD runs using Exactive Orbitrap MS system. An approximate 10x increase is observed with addition of each counter electrode.

34  
35  
36  
37  
38  
39  
40  
41  
Figure 7. Photograph of quad-electrode LS-APGD ion source, showing 4 counter electrodes in vertical axis, along with horizontal solution electrode and ion sampling capillary of PNNL/EMSL Exactive Orbitrap MS.

1  
2  
3  
4  
5  
6  
7  
8  
9  
10  
11  
12  
13  
14  
15  
16  
17  
18  
19  
20  
21  
22  
23  
24  
25  
26  
27  
28  
29  
30  
31  
32  
33  
34  
35  
36  
37

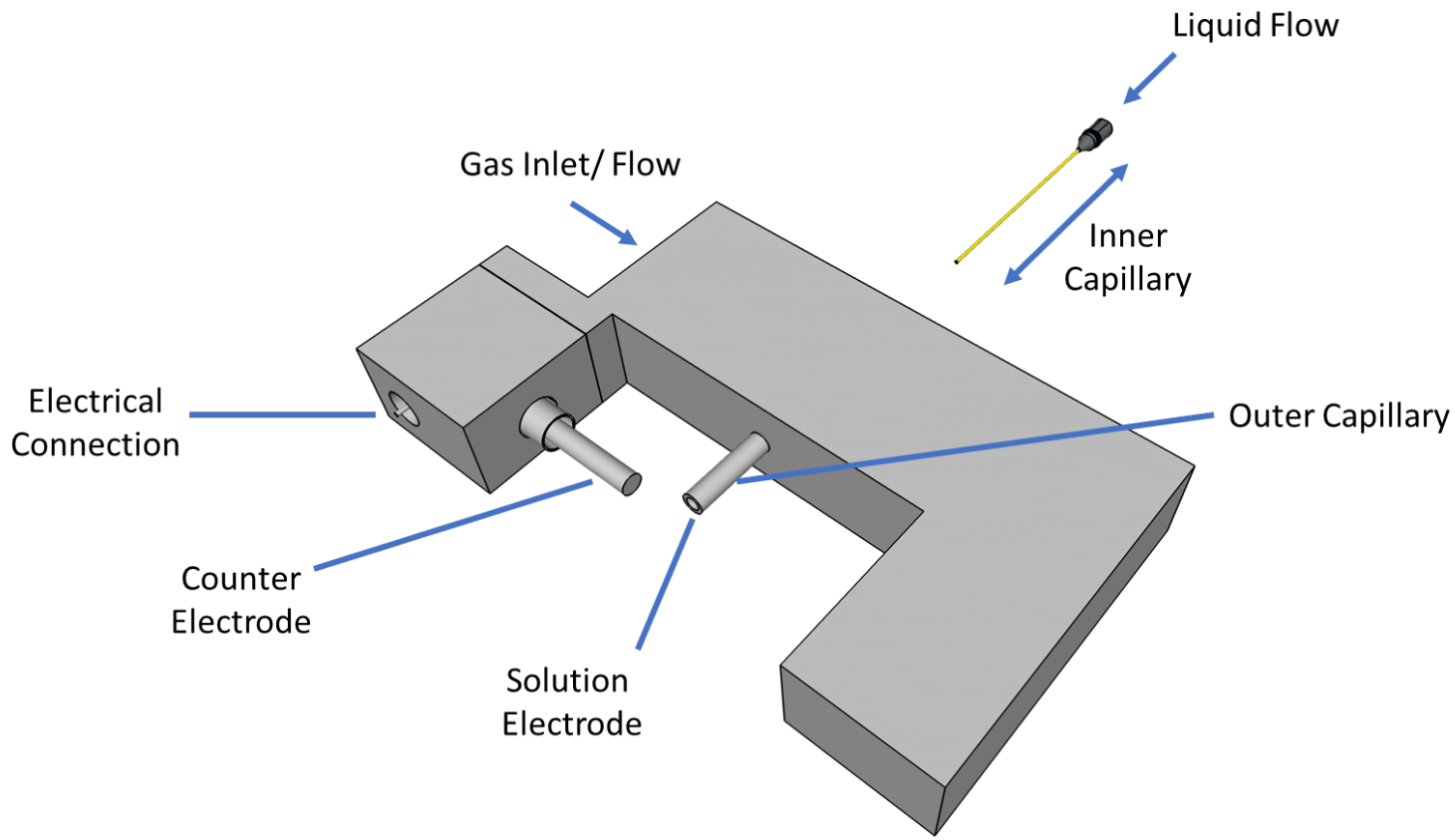
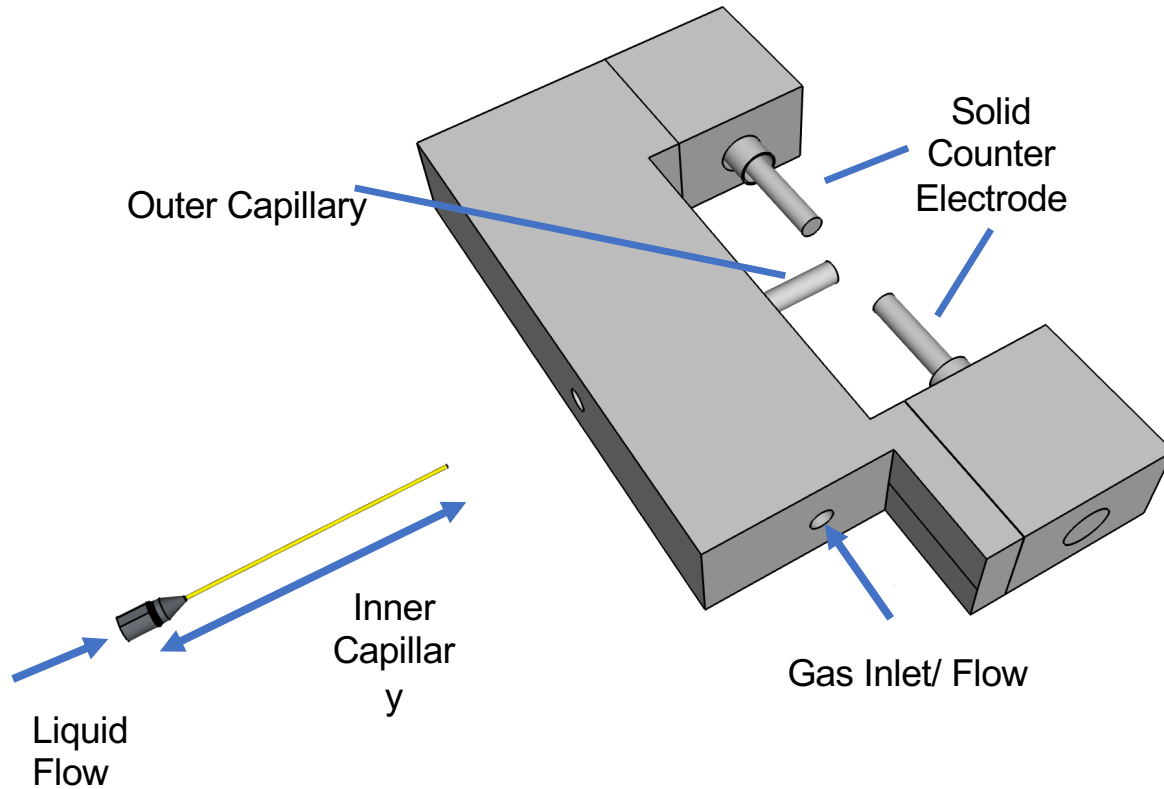


Figure 1a



1  
2  
3  
4  
5  
6  
7  
8  
9  
10  
11  
12  
13  
14  
15  
16  
17  
18  
19  
20  
21  
22  
23  
24  
25  
26  
27  
28  
29  
30  
31  
32  
33  
34  
35  
36  
37  
38  
39  
40  
41  
42  
43  
44  
45  
46  
47  
48  
49  
50  
51  
52  
53  
54  
55  
56  
57  
58  
59  
60  
61  
62  
63  
64  
65  
66  
67  
68  
69  
70  
71  
72  
73  
74  
75  
76  
77  
78  
79  
80  
81  
82  
83  
84  
85  
86  
87  
88  
89  
90  
91  
92  
93  
94  
95  
96  
97  
98  
99  
100  
101  
102  
103  
104  
105  
106  
107  
108  
109  
110  
111  
112  
113  
114  
115  
116  
117  
118  
119  
120  
121  
122  
123  
124  
125  
126  
127  
128  
129  
130  
131  
132  
133  
134  
135  
136  
137  
138  
139  
140  
141  
142  
143  
144  
145  
146  
147  
148  
149  
150  
151  
152  
153  
154  
155  
156  
157  
158  
159  
160  
161  
162  
163  
164  
165  
166  
167  
168  
169  
170  
171  
172  
173  
174  
175  
176  
177  
178  
179  
180  
181  
182  
183  
184  
185  
186  
187  
188  
189  
190  
191  
192  
193  
194  
195  
196  
197  
198  
199  
200  
201  
202  
203  
204  
205  
206  
207  
208  
209  
210  
211  
212  
213  
214  
215  
216  
217  
218  
219  
220  
221  
222  
223  
224  
225  
226  
227  
228  
229  
230  
231  
232  
233  
234  
235  
236  
237  
238  
239  
240  
241  
242  
243  
244  
245  
246  
247  
248  
249  
250  
251  
252  
253  
254  
255  
256  
257  
258  
259  
260  
261  
262  
263  
264  
265  
266  
267  
268  
269  
270  
271  
272  
273  
274  
275  
276  
277  
278  
279  
280  
281  
282  
283  
284  
285  
286  
287  
288  
289  
290  
291  
292  
293  
294  
295  
296  
297  
298  
299  
300  
301  
302  
303  
304  
305  
306  
307  
308  
309  
310  
311  
312  
313  
314  
315  
316  
317  
318  
319  
320  
321  
322  
323  
324  
325  
326  
327  
328  
329  
330  
331  
332  
333  
334  
335  
336  
337  
338  
339  
340  
341  
342  
343  
344  
345  
346  
347  
348  
349  
350  
351  
352  
353  
354  
355  
356  
357  
358  
359  
360  
361  
362  
363  
364  
365  
366  
367  
368  
369  
370  
371  
372  
373  
374  
375  
376  
377  
378  
379  
380  
381  
382  
383  
384  
385  
386  
387  
388  
389  
390  
391  
392  
393  
394  
395  
396  
397  
398  
399  
400  
401  
402  
403  
404  
405  
406  
407  
408  
409  
410  
411  
412  
413  
414  
415  
416  
417  
418  
419  
420  
421  
422  
423  
424  
425  
426  
427  
428  
429  
430  
431  
432  
433  
434  
435  
436  
437  
438  
439  
440  
441  
442  
443  
444  
445  
446  
447  
448  
449  
450  
451  
452  
453  
454  
455  
456  
457  
458  
459  
460  
461  
462  
463  
464  
465  
466  
467  
468  
469  
470  
471  
472  
473  
474  
475  
476  
477  
478  
479  
480  
481  
482  
483  
484  
485  
486  
487  
488  
489  
490  
491  
492  
493  
494  
495  
496  
497  
498  
499  
500

Figure 1b

1  
2  
3  
4  
5  
6  
7  
8  
9  
10  
11  
12  
13  
14  
15  
16  
17  
18  
19  
20  
21  
22  
23  
24  
25  
26  
27  
28  
29  
30  
31  
32  
33  
34  
35  
36  
37  
38  
39  
40  
41  
42  
43  
44  
45  
46  
47  
48  
49  
50  
51  
52  
53  
54  
55  
56  
57  
58  
59  
60  
61  
62  
63  
64  
65  
66  
67  
68  
69  
70  
71  
72  
73  
74  
75  
76  
77  
78  
79  
80  
81  
82  
83  
84  
85  
86  
87  
88  
89  
90  
91  
92  
93  
94  
95  
96  
97  
98  
99  
100  
101  
102  
103  
104  
105  
106  
107  
108  
109  
110  
111  
112  
113  
114  
115  
116  
117  
118  
119  
120  
121  
122  
123  
124  
125  
126  
127  
128  
129  
130  
131  
132  
133  
134  
135  
136  
137  
138  
139  
140  
141  
142  
143  
144  
145  
146  
147  
148  
149  
150  
151  
152  
153  
154  
155  
156  
157  
158  
159  
160  
161  
162  
163  
164  
165  
166  
167  
168  
169  
170  
171  
172  
173  
174  
175  
176  
177  
178  
179  
180  
181  
182  
183  
184  
185  
186  
187  
188  
189  
190  
191  
192  
193  
194  
195  
196  
197  
198  
199  
200  
201  
202  
203  
204  
205  
206  
207  
208  
209  
210  
211  
212  
213  
214  
215  
216  
217  
218  
219  
220  
221  
222  
223  
224  
225  
226  
227  
228  
229  
230  
231  
232  
233  
234  
235  
236  
237  
238  
239  
240  
241  
242  
243  
244  
245  
246  
247  
248  
249  
250  
251  
252  
253  
254  
255  
256  
257  
258  
259  
260  
261  
262  
263  
264  
265  
266  
267  
268  
269  
270  
271  
272  
273  
274  
275  
276  
277  
278  
279  
280  
281  
282  
283  
284  
285  
286  
287  
288  
289  
290  
291  
292  
293  
294  
295  
296  
297  
298  
299  
300  
301  
302  
303  
304  
305  
306  
307  
308  
309  
310  
311  
312  
313  
314  
315  
316  
317  
318  
319  
320  
321  
322  
323  
324  
325  
326  
327  
328  
329  
330  
331  
332  
333  
334  
335  
336  
337  
338  
339  
340  
341  
342  
343  
344  
345  
346  
347  
348  
349  
350  
351  
352  
353  
354  
355  
356  
357  
358  
359  
360  
361  
362  
363  
364  
365  
366  
367  
368  
369  
370  
371  
372  
373  
374  
375  
376  
377  
378  
379  
380  
381  
382  
383  
384  
385  
386  
387  
388  
389  
390  
391  
392  
393  
394  
395  
396  
397  
398  
399  
400  
401  
402  
403  
404  
405  
406  
407  
408  
409  
410  
411  
412  
413  
414  
415  
416  
417  
418  
419  
420  
421  
422  
423  
424  
425  
426  
427  
428  
429  
430  
431  
432  
433  
434  
435  
436  
437  
438  
439  
440  
441  
442  
443  
444  
445  
446  
447  
448  
449  
450  
451  
452  
453  
454  
455  
456  
457  
458  
459  
460  
461  
462  
463  
464  
465  
466  
467  
468  
469  
470  
471  
472  
473  
474  
475  
476  
477  
478  
479  
480  
481  
482  
483  
484  
485  
486  
487  
488  
489  
490  
491  
492  
493  
494  
495  
496  
497  
498  
499  
500

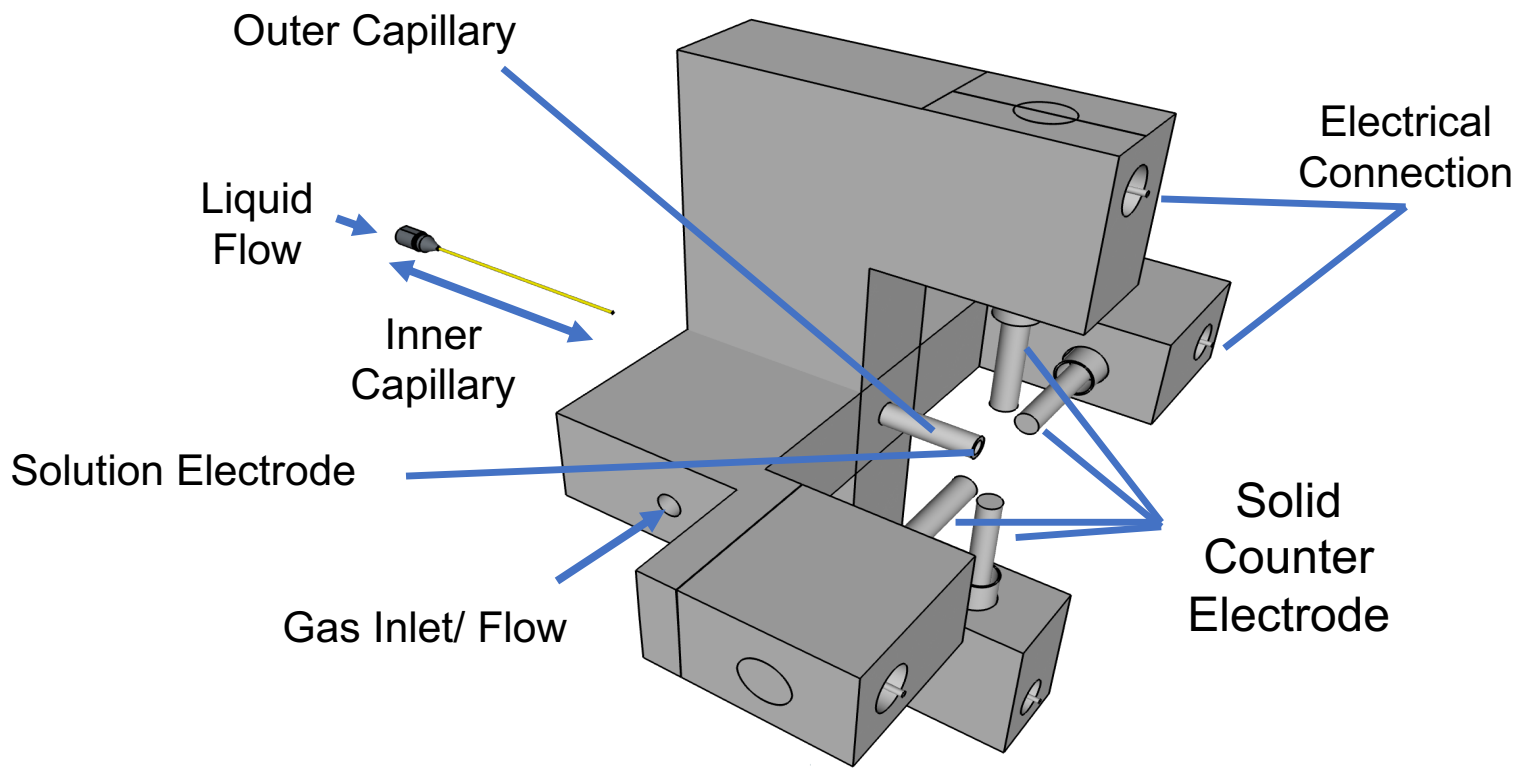


Figure 10

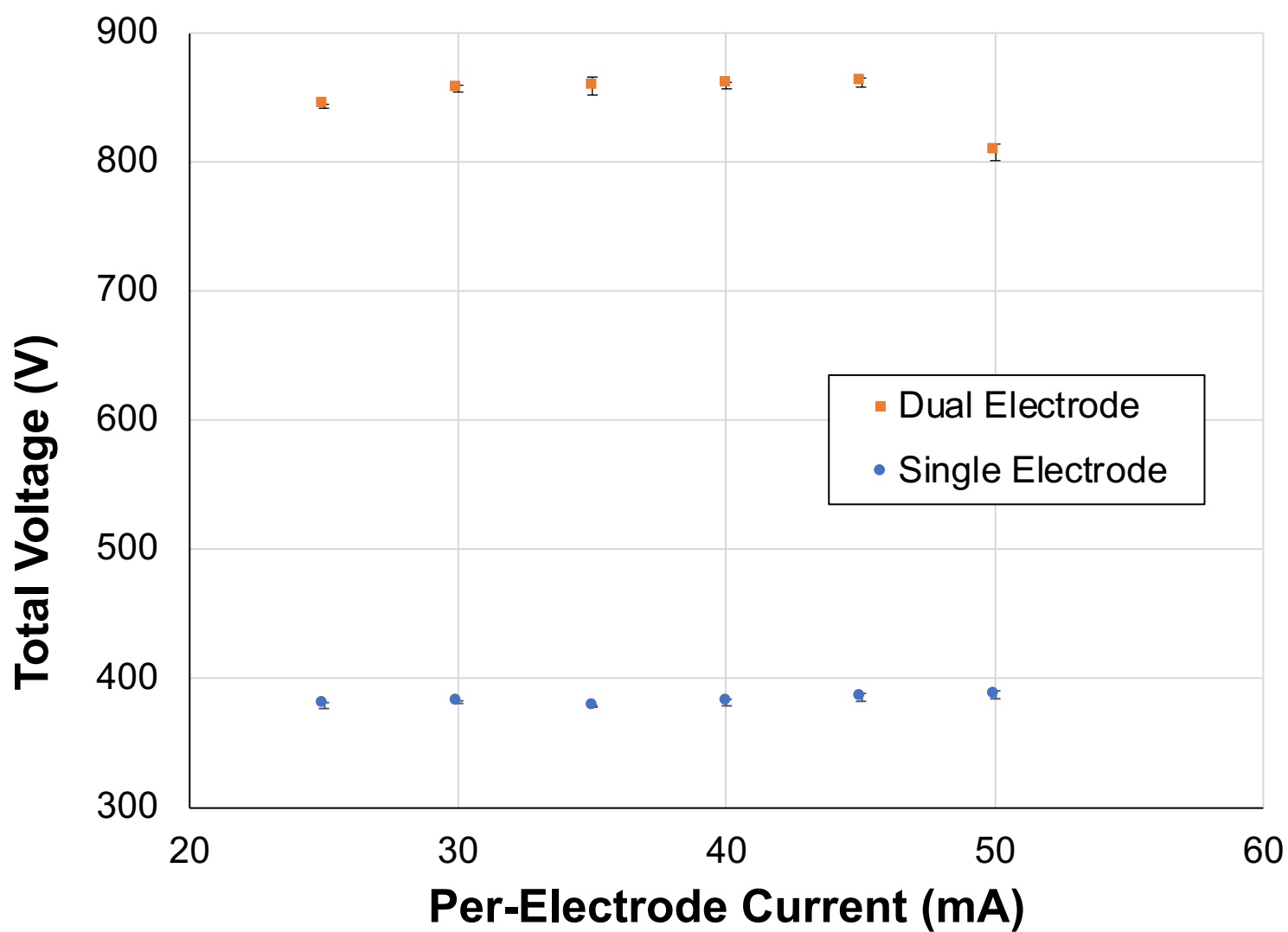
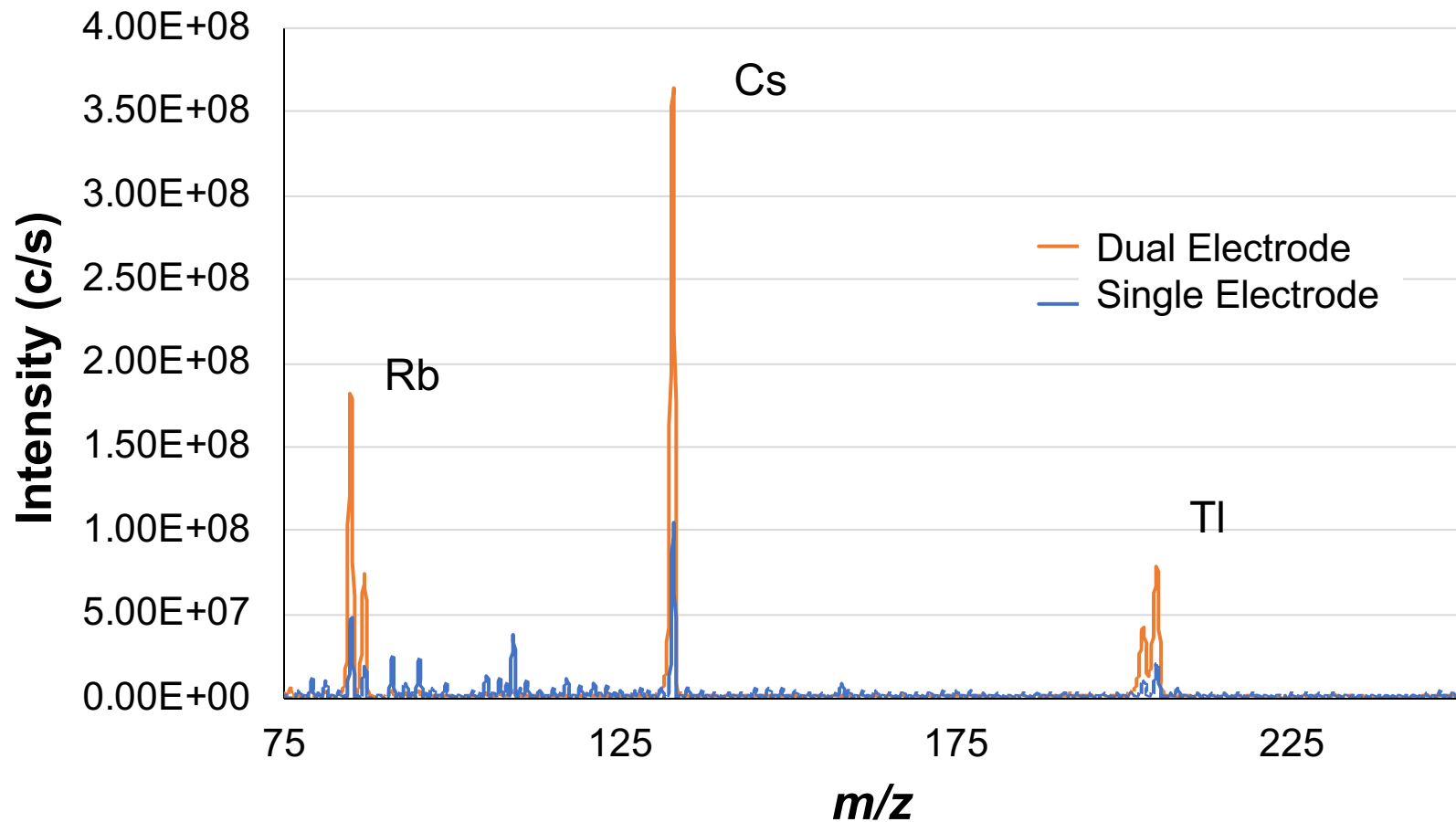
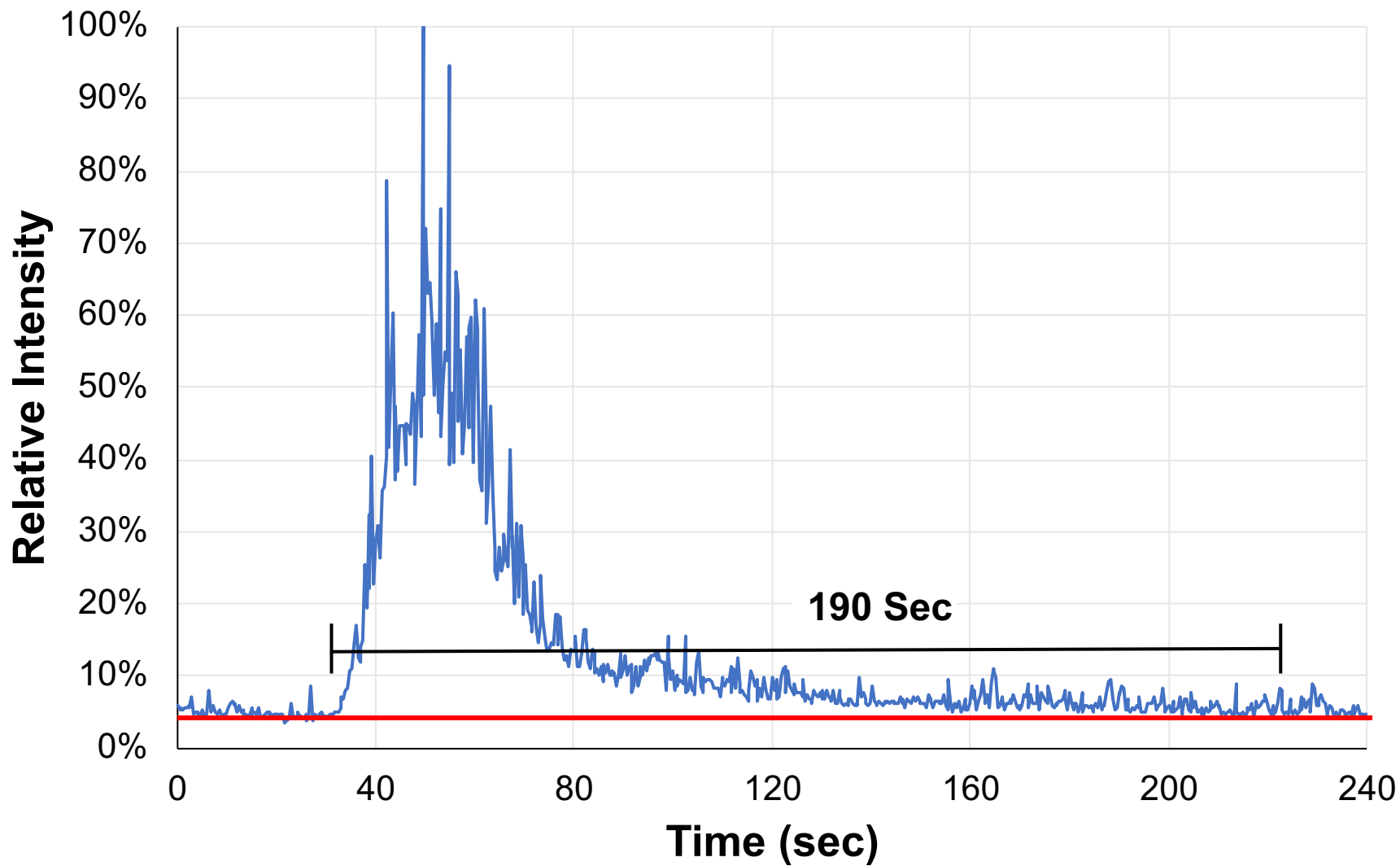
1  
2  
3  
4  
5  
6  
7  
8  
9  
10  
11  
12  
13  
14  
15  
16  
17  
18  
19  
20  
21  
22  
23  
24  
25  
26  
27  
28  
29  
30  
31  
32  
33  
34  
35  
36  
37  
38  
39  
40  
41  
42  
43  
44  
45  
46  
47  
48  
49  
50  
51  
52  
53  
54  
55  
56  
57  
58  
59  
60  
61  
62  
63  
64  
65  
66  
67  
68  
69  
70  
71  
72  
73  
74  
75  
76  
77  
78  
79  
80  
81  
82  
83  
84  
85  
86  
87  
88  
89  
90  
91  
92  
93  
94  
95  
96  
97  
98  
99  
100  
101  
102  
103  
104  
105  
106  
107  
108  
109  
110  
111  
112  
113  
114  
115  
116  
117  
118  
119  
120  
121  
122  
123  
124  
125  
126  
127  
128  
129  
130  
131  
132  
133  
134  
135  
136  
137  
138  
139  
140  
141  
142  
143  
144  
145  
146  
147  
148  
149  
150  
151  
152  
153  
154  
155  
156  
157  
158  
159  
160  
161  
162  
163  
164  
165  
166  
167  
168  
169  
170  
171  
172  
173  
174  
175  
176  
177  
178  
179  
180  
181  
182  
183  
184  
185  
186  
187  
188  
189  
190  
191  
192  
193  
194  
195  
196  
197  
198  
199  
200  
201  
202  
203  
204  
205  
206  
207  
208  
209  
210  
211  
212  
213  
214  
215  
216  
217  
218  
219  
220  
221  
222  
223  
224  
225  
226  
227  
228  
229  
230  
231  
232  
233  
234  
235  
236  
237  
238  
239  
240  
241  
242  
243  
244  
245  
246  
247  
248  
249  
250  
251  
252  
253  
254  
255  
256  
257  
258  
259  
260  
261  
262  
263  
264  
265  
266  
267  
268  
269  
270  
271  
272  
273  
274  
275  
276  
277  
278  
279  
280  
281  
282  
283  
284  
285  
286  
287  
288  
289  
290  
291  
292  
293  
294  
295  
296  
297  
298  
299  
300  
301  
302  
303  
304  
305  
306  
307  
308  
309  
310  
311  
312  
313  
314  
315  
316  
317  
318  
319  
320  
321  
322  
323  
324  
325  
326  
327  
328  
329  
330  
331  
332  
333  
334  
335  
336  
337  
338  
339  
340  
341  
342  
343  
344  
345  
346  
347  
348  
349  
350  
351  
352  
353  
354  
355  
356  
357  
358  
359  
360  
361  
362  
363  
364  
365  
366  
367  
368  
369  
370  
371  
372  
373  
374  
375  
376  
377  
378  
379  
380  
381  
382  
383  
384  
385  
386  
387  
388  
389  
390  
391  
392  
393  
394  
395  
396  
397  
398  
399  
400  
401  
402  
403  
404  
405  
406  
407  
408  
409  
410  
411  
412  
413  
414  
415  
416  
417  
418  
419  
420  
421  
422  
423  
424  
425  
426  
427  
428  
429  
430  
431  
432  
433  
434  
435  
436  
437  
438  
439  
440  
441  
442  
443  
444  
445  
446  
447  
448  
449  
450  
451  
452  
453  
454  
455  
456  
457  
458  
459  
460  
461  
462  
463  
464  
465  
466  
467  
468  
469  
470  
471  
472  
473  
474  
475  
476  
477  
478  
479  
480  
481  
482  
483  
484  
485  
486  
487  
488  
489  
490  
491  
492  
493  
494  
495  
496  
497  
498  
499  
500  
501  
502  
503  
504  
505  
506  
507  
508  
509  
510  
511  
512  
513  
514  
515  
516  
517  
518  
519  
520  
521  
522  
523  
524  
525  
526  
527  
528  
529  
530  
531  
532  
533  
534  
535  
536  
537  
538  
539  
540  
541  
542  
543  
544  
545  
546  
547  
548  
549  
550  
551  
552  
553  
554  
555  
556  
557  
558  
559  
560  
561  
562  
563  
564  
565  
566  
567  
568  
569  
570  
571  
572  
573  
574  
575  
576  
577  
578  
579  
580  
581  
582  
583  
584  
585  
586  
587  
588  
589  
590  
591  
592  
593  
594  
595  
596  
597  
598  
599  
600  
601  
602  
603  
604  
605  
606  
607  
608  
609  
610  
611  
612  
613  
614  
615  
616  
617  
618  
619  
620  
621  
622  
623  
624  
625  
626  
627  
628  
629  
630  
631  
632  
633  
634  
635  
636  
637  
638  
639  
640  
641  
642  
643  
644  
645  
646  
647  
648  
649  
650  
651  
652  
653  
654  
655  
656  
657  
658  
659  
660  
661  
662  
663  
664  
665  
666  
667  
668  
669  
670  
671  
672  
673  
674  
675  
676  
677  
678  
679  
680  
681  
682  
683  
684  
685  
686  
687  
688  
689  
690  
691  
692  
693  
694  
695  
696  
697  
698  
699  
700  
701  
702  
703  
704  
705  
706  
707  
708  
709  
710  
711  
712  
713  
714  
715  
716  
717  
718  
719  
720  
721  
722  
723  
724  
725  
726  
727  
728  
729  
730  
731  
732  
733  
734  
735  
736  
737  
738  
739  
740  
741  
742  
743  
744  
745  
746  
747  
748  
749  
750  
751  
752  
753  
754  
755  
756  
757  
758  
759  
760  
761  
762  
763  
764  
765  
766  
767  
768  
769  
770  
771  
772  
773  
774  
775  
776  
777  
778  
779  
780  
781  
782  
783  
784  
785  
786  
787  
788  
789  
790  
791  
792  
793  
794  
795  
796  
797  
798  
799  
800  
801  
802  
803  
804  
805  
806  
807  
808  
809  
810  
811  
812  
813  
814  
815  
816  
817  
818  
819  
820  
821  
822  
823  
824  
825  
826  
827  
828  
829  
830  
831  
832  
833  
834  
835  
836  
837  
838  
839  
840  
841  
842  
843  
844  
845  
846  
847  
848  
849  
850  
851  
852  
853  
854  
855  
856  
857  
858  
859  
860  
861  
862  
863  
864  
865  
866  
867  
868  
869  
870  
871  
872  
873  
874  
875  
876  
877  
878  
879  
880  
881  
882  
883  
884  
885  
886  
887  
888  
889  
890  
891  
892  
893  
894  
895  
896  
897  
898  
899  
900  
901  
902  
903  
904  
905  
906  
907  
908  
909  
910  
911  
912  
913  
914  
915  
916  
917  
918  
919  
920  
921  
922  
923  
924  
925  
926  
927  
928  
929  
930  
931  
932  
933  
934  
935  
936  
937  
938  
939  
940  
941  
942  
943  
944  
945  
946  
947  
948  
949  
950  
951  
952  
953  
954  
955  
956  
957  
958  
959  
960  
961  
962  
963  
964  
965  
966  
967  
968  
969  
970  
971  
972  
973  
974  
975  
976  
977  
978  
979  
980  
981  
982  
983  
984  
985  
986  
987  
988  
989  
990  
991  
992  
993  
994  
995  
996  
997  
998  
999  
1000

Figure 2



1  
2  
3  
4  
5  
6  
7  
8  
9  
10  
11  
12  
13  
14  
15  
16  
17  
18  
19  
20  
21  
22  
23  
24  
25  
26  
27  
28  
29  
30  
31  
32  
33  
34  
35  
36  
37  
38  
39  
40  
41  
42  
43  
44  
45  
46  
47  
48  
49  
50  
51  
52  
53  
54  
55  
56  
57  
58  
59  
60  
61  
62  
63  
64  
65  
66  
67  
68  
69  
70  
71  
72  
73  
74  
75  
76  
77  
78  
79  
80  
81  
82  
83  
84  
85  
86  
87  
88  
89  
90  
91  
92  
93  
94  
95  
96  
97  
98  
99  
100

Figure 3



1  
2  
3  
4  
5  
6  
7  
8  
9  
10  
11  
12  
13  
14  
15  
16  
17  
18  
19  
20  
21  
22  
23  
24  
25  
26  
27  
28  
29  
30  
31  
32  
33  
34  
35  
36  
37  
38  
39  
40  
41  
42  
43  
44  
45  
46  
47  
48  
49  
50  
51  
52  
53  
54  
55  
56  
57  
58  
59  
60  
61  
62  
63  
64  
65  
66  
67  
68  
69  
70  
71  
72  
73  
74  
75  
76  
77  
78  
79  
80  
81  
82  
83  
84  
85  
86  
87  
88  
89  
90  
91  
92  
93  
94  
95  
96  
97  
98  
99  
100  
101  
102  
103  
104  
105  
106  
107  
108  
109  
110  
111  
112  
113  
114  
115  
116  
117  
118  
119  
120  
121  
122  
123  
124  
125  
126  
127  
128  
129  
130  
131  
132  
133  
134  
135  
136  
137  
138  
139  
140  
141  
142  
143  
144  
145  
146  
147  
148  
149  
150  
151  
152  
153  
154  
155  
156  
157  
158  
159  
160  
161  
162  
163  
164  
165  
166  
167  
168  
169  
170  
171  
172  
173  
174  
175  
176  
177  
178  
179  
180  
181  
182  
183  
184  
185  
186  
187  
188  
189  
190  
191  
192  
193  
194  
195  
196  
197  
198  
199  
200  
201  
202  
203  
204  
205  
206  
207  
208  
209  
210  
211  
212  
213  
214  
215  
216  
217  
218  
219  
220  
221  
222  
223  
224  
225  
226  
227  
228  
229  
230  
231  
232  
233  
234  
235  
236  
237  
238  
239  
240  
241  
242  
243  
244  
245  
246  
247  
248  
249  
250  
251  
252  
253  
254  
255  
256  
257  
258  
259  
260  
261  
262  
263  
264  
265  
266  
267  
268  
269  
270  
271  
272  
273  
274  
275  
276  
277  
278  
279  
280  
281  
282  
283  
284  
285  
286  
287  
288  
289  
290  
291  
292  
293  
294  
295  
296  
297  
298  
299  
300  
301  
302  
303  
304  
305  
306  
307  
308  
309  
310  
311  
312  
313  
314  
315  
316  
317  
318  
319  
320  
321  
322  
323  
324  
325  
326  
327  
328  
329  
330  
331  
332  
333  
334  
335  
336  
337  
338  
339  
340  
341  
342  
343  
344  
345  
346  
347  
348  
349  
350  
351  
352  
353  
354  
355  
356  
357  
358  
359  
360  
361  
362  
363  
364  
365  
366  
367  
368  
369  
370  
371  
372  
373  
374  
375  
376  
377  
378  
379  
380  
381  
382  
383  
384  
385  
386  
387  
388  
389  
390  
391  
392  
393  
394  
395  
396  
397  
398  
399  
400  
401  
402  
403  
404  
405  
406  
407  
408  
409  
410  
411  
412  
413  
414  
415  
416  
417  
418  
419  
420  
421  
422  
423  
424  
425  
426  
427  
428  
429  
430  
431  
432  
433  
434  
435  
436  
437  
438  
439  
440  
441  
442  
443  
444  
445  
446  
447  
448  
449  
450  
451  
452  
453  
454  
455  
456  
457  
458  
459  
460  
461  
462  
463  
464  
465  
466  
467  
468  
469  
470  
471  
472  
473  
474  
475  
476  
477  
478  
479  
480  
481  
482  
483  
484  
485  
486  
487  
488  
489  
490  
491  
492  
493  
494  
495  
496  
497  
498  
499  
500

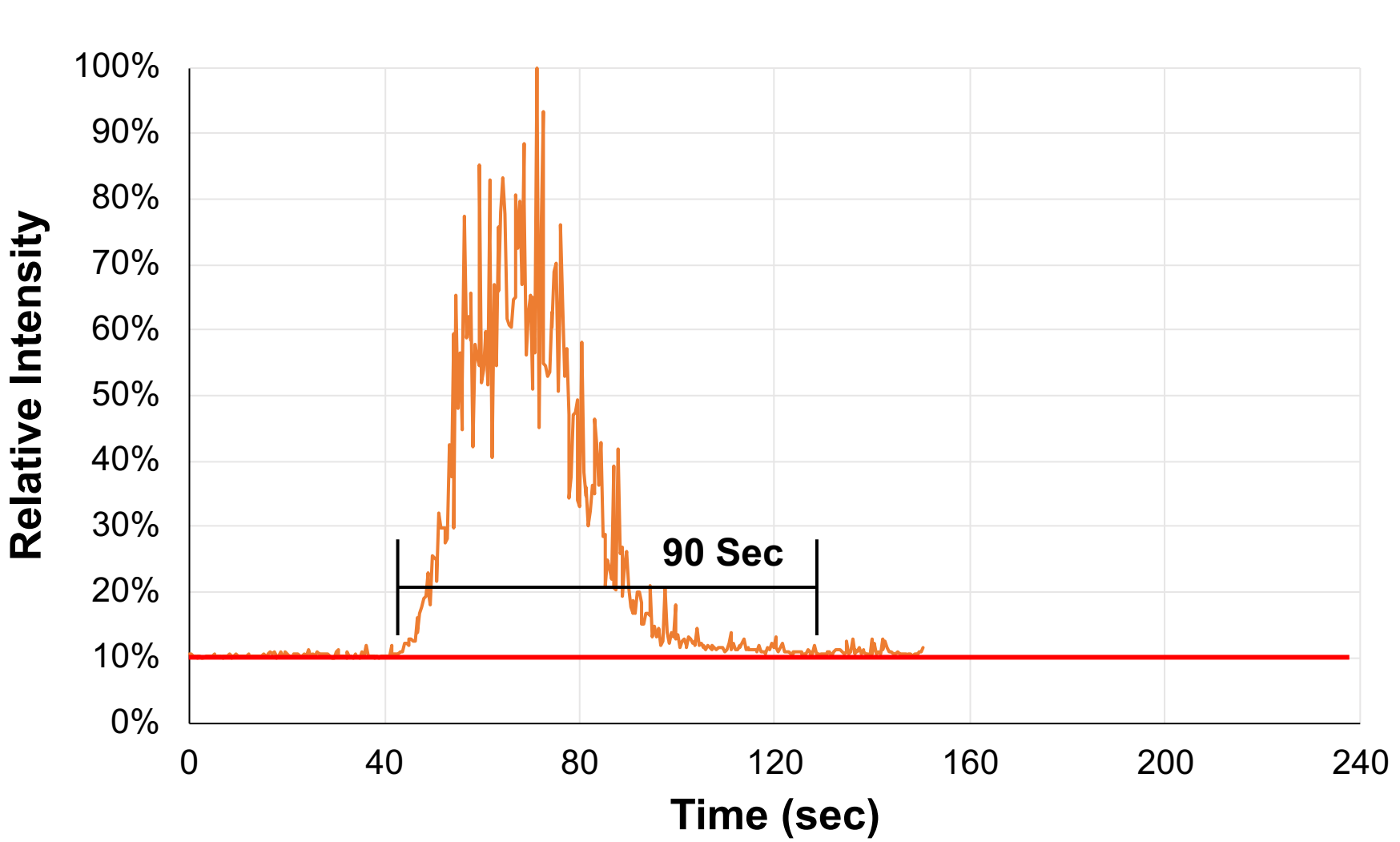
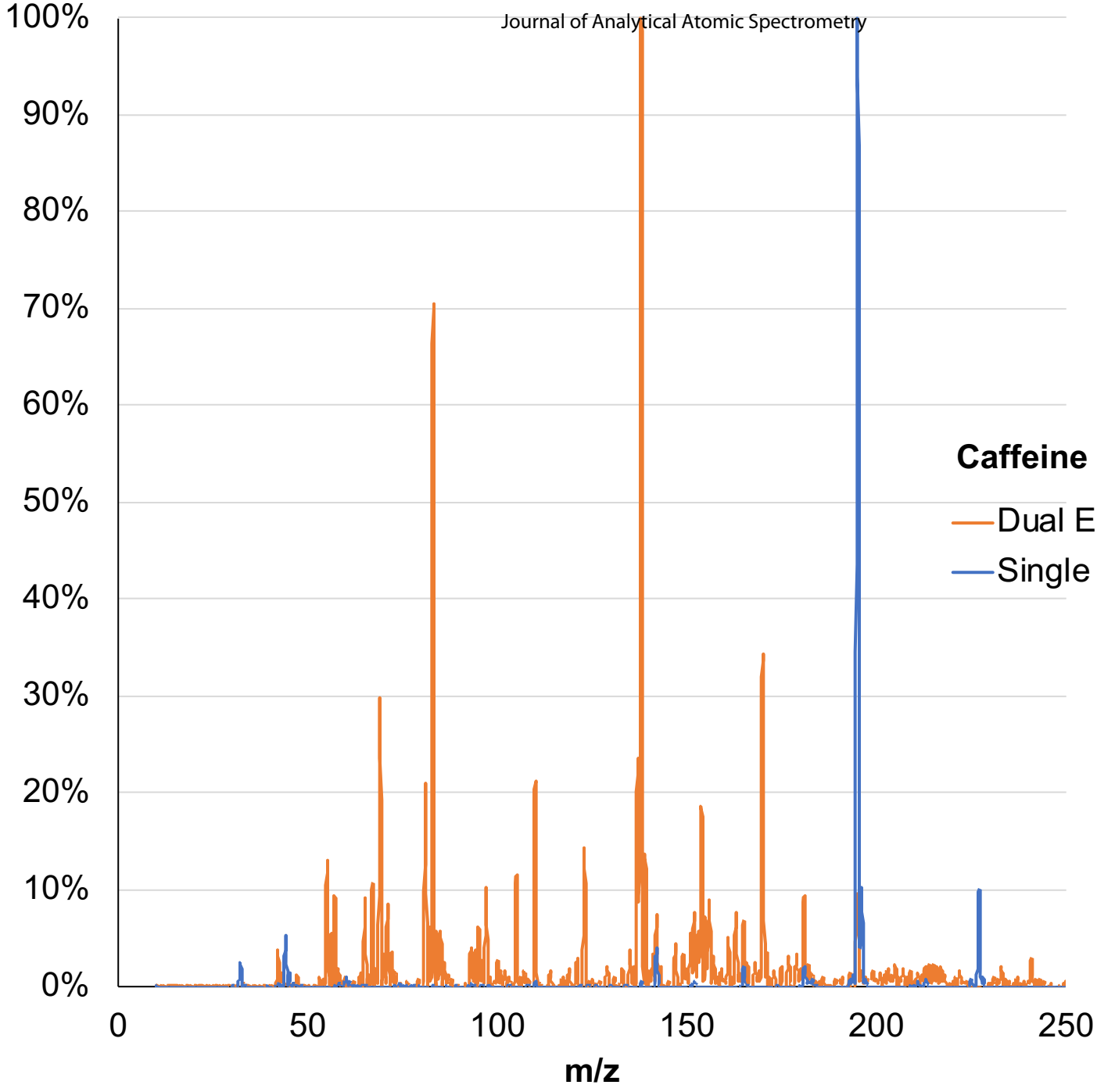


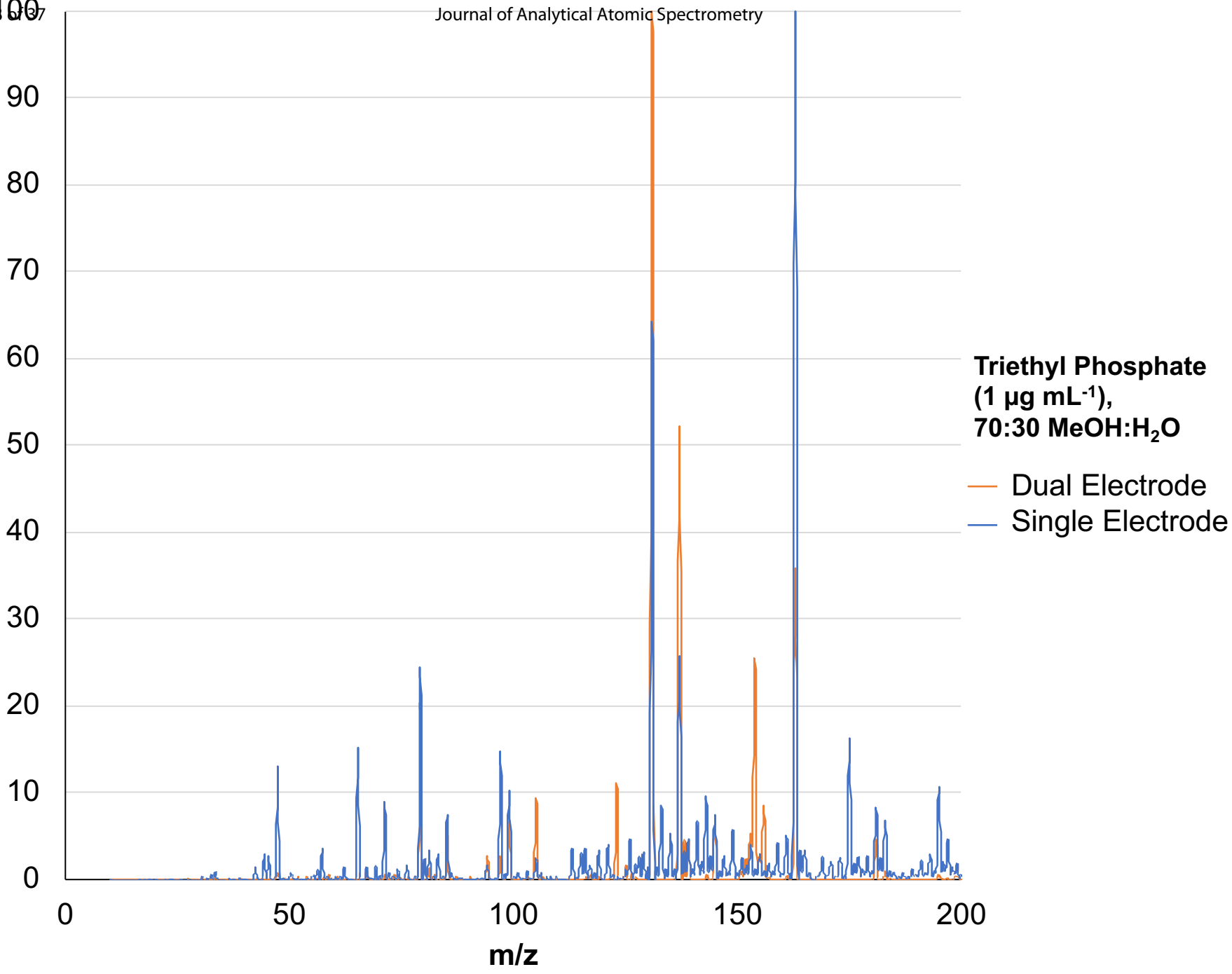
Figure 4B

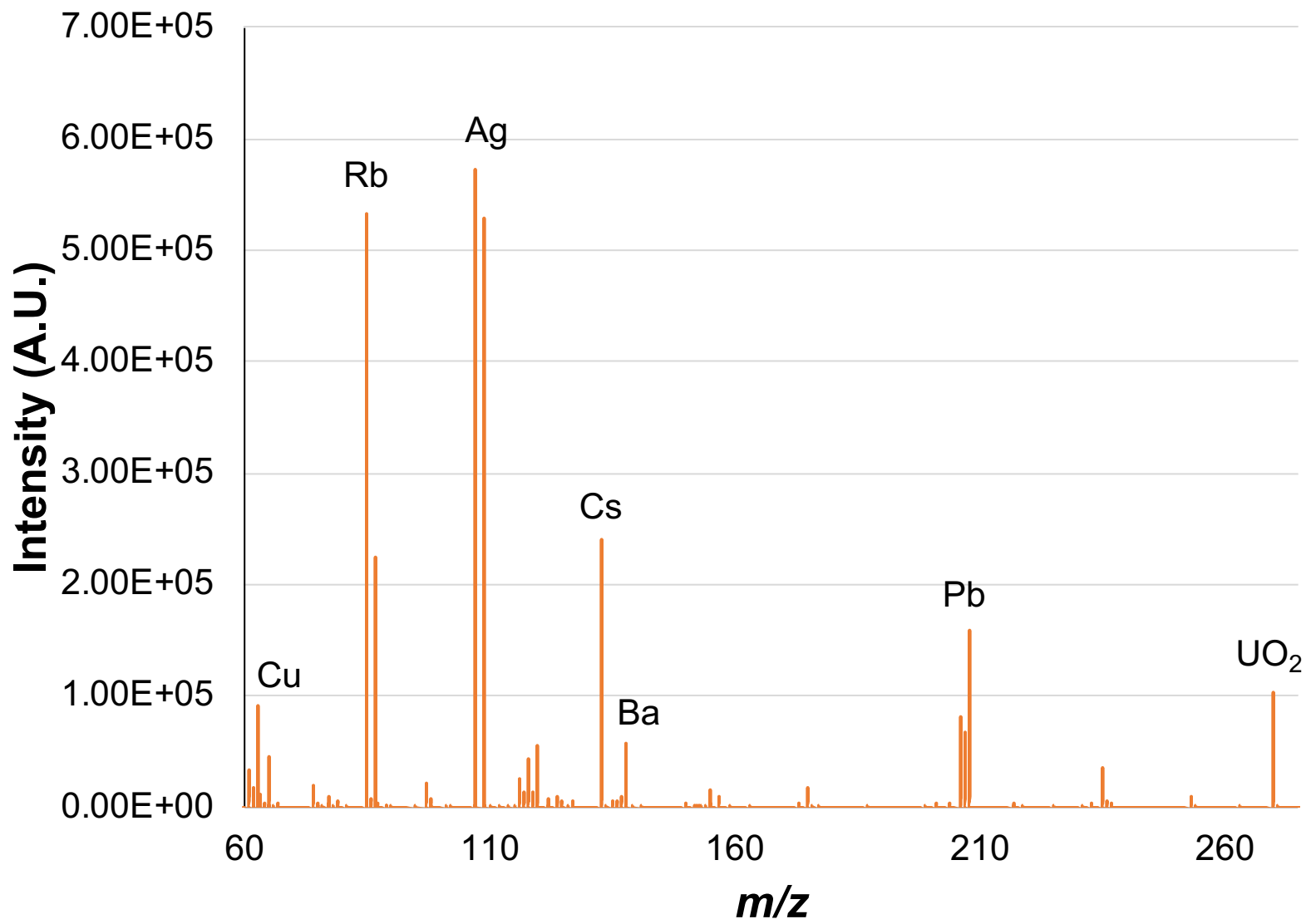
1  
2  
3  
4  
5  
6  
7  
8  
9  
10  
11  
12  
13  
14  
15  
16  
17  
18  
19  
20  
21  
22  
23  
24  
25  
26  
27  
28  
29  
30  
31  
32  
33  
34  
35  
36  
37  
38  
39  
40  
Figure 5A

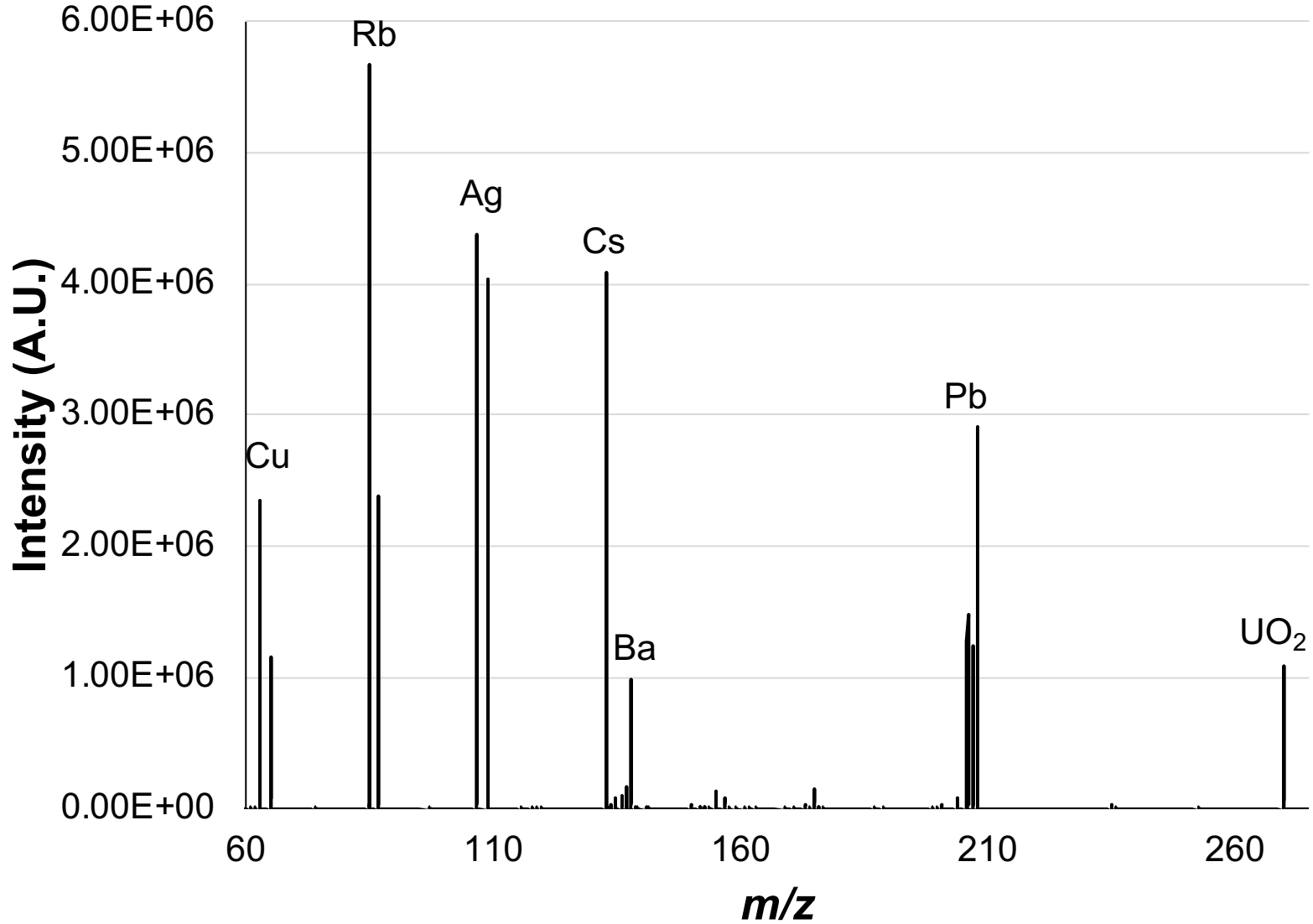


**Caffeine**  
— Dual Electrode  
— Single Electrode

1  
2  
3  
4  
5  
6  
7  
8  
9  
10  
11  
12  
13  
14  
15  
16  
17  
18  
19  
20  
21  
22  
23  
24  
25  
26  
27  
28  
29  
30  
31  
32  
33  
34  
35  
36  
37  
38  
39  
40  
Figure 5B

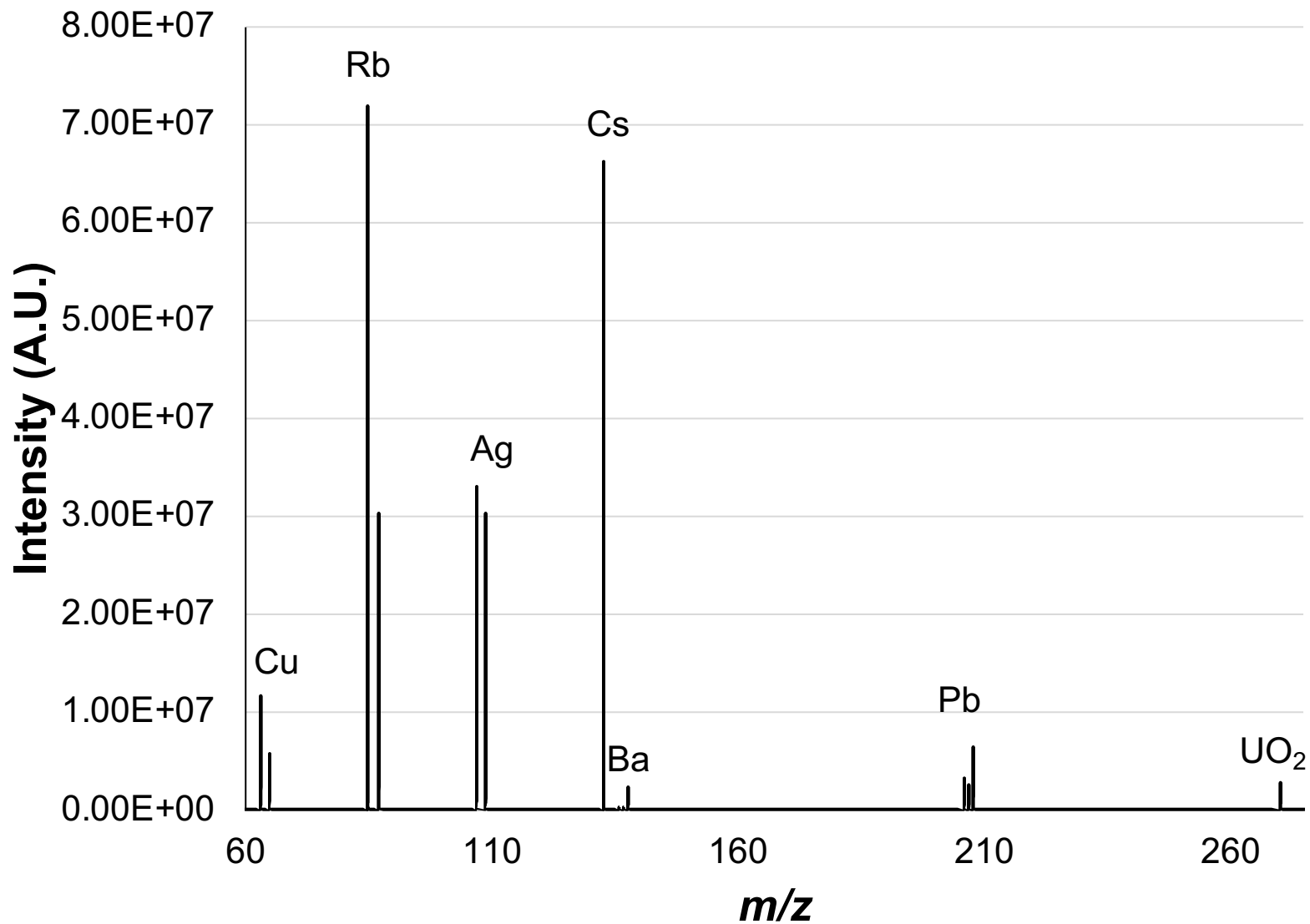






1  
2  
3  
4  
5  
6  
7  
8  
9  
10  
11  
12  
13  
14  
15  
16  
17  
18  
19  
20  
21  
22  
23  
24  
25  
26  
27  
28  
29  
30  
31  
32  
33  
34  
35  
36  
37  
38  
39  
40  
41  
42  
43  
44  
45  
46  
47  
48  
49  
50  
51  
52  
53  
54  
55  
56  
57  
58  
59  
60  
61  
62  
63  
64  
65  
66  
67  
68  
69  
70  
71  
72  
73  
74  
75  
76  
77  
78  
79  
80  
81  
82  
83  
84  
85  
86  
87  
88  
89  
90  
91  
92  
93  
94  
95  
96  
97  
98  
99  
100

Figure 6b



1  
2  
3  
4  
5  
6  
7  
8  
9  
10  
11  
12  
13  
14  
15  
16  
17  
18  
19  
20  
21  
22  
23  
24  
25  
26  
27  
28  
29  
30  
31  
32  
33  
34  
35  
36

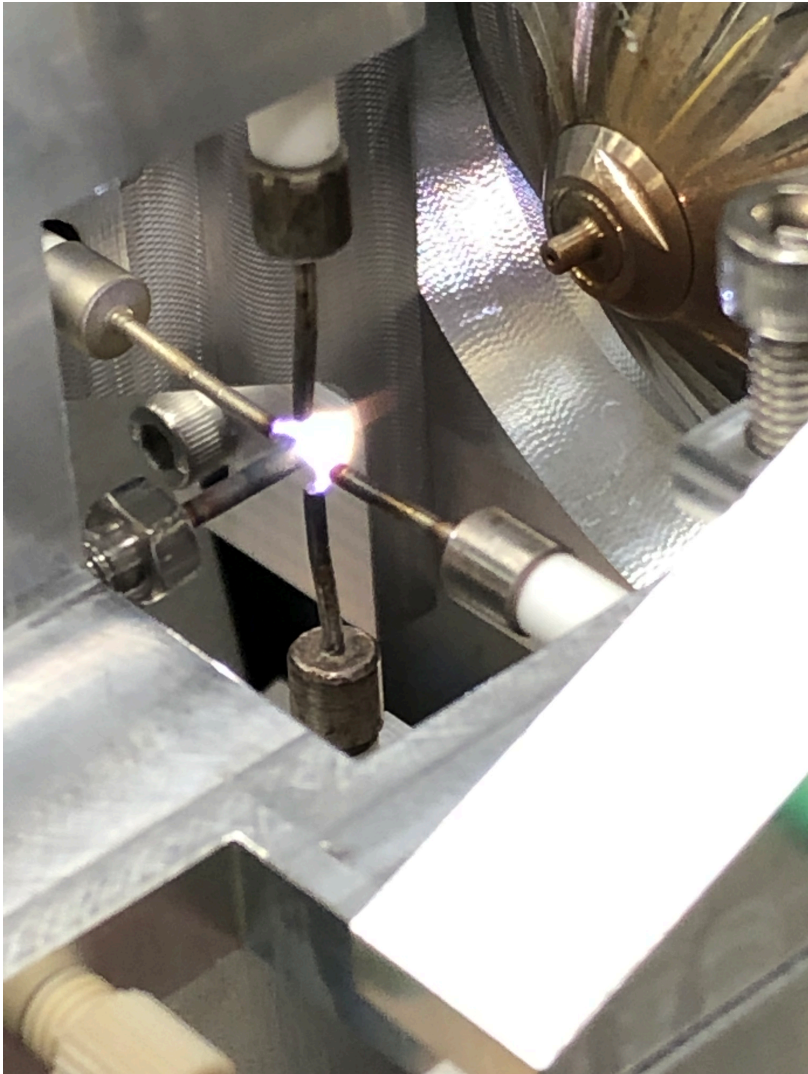


Figure 7